IEEE STANDARDS ASSOCIATION

IEEE Guide for Determining Fault Location on AC Transmission and Distribution Lines

IEEE Power and Energy Society

Sponsored by the
Power System Relaying Committee

IEEE
3 Park Avenue
New York, NY 10016-5997
USA

IEEE Std C37.114™-2014
(Revision of
IEEE Std C37.114-2004)

IEEE Std C37.114™-2014
(Revision of
IEEE Std C37.114-2004)

IEEE Guide for Determining Fault Location on AC Transmission and Distribution Lines

Sponsor

Power System Relaying Committee
of the
IEEE Power and Energy Society

Approved 10 December 2014

IEEE-SA Standards Board

Abstract: Electrical faults on transmission and distribution lines are detected and isolated by system protective devices. Once the fault has been cleared, outage times can be reduced if the location of the fault can be determined more quickly. The techniques and application considerations for determining the location of a fault on ac transmission and distribution lines are outlined in this guide. Traditional approaches and the primary measurement techniques used in modern devices are reviewed: one- and two-terminal impedance-based methods and traveling-wave methods. Application considerations include: two- and three-terminal lines, series-compensated lines, parallel lines, untransposed lines, underground cables, fault resistance effects, and other power system conditions, including those unique to distribution systems.

Keywords: fault location, IEEE C37.114™, relays, synchrophasor, system protection, travelling waves

The Institute of Electrical and Electronics Engineers, Inc.
3 Park Avenue, New York, NY 10016-5997, USA

PDF: ISBN 978-0-7381-9421-9 STD20037
Print: ISBN 978-0-7381-9422-6 STDPD20037

Important Notices and Disclaimers Concerning IEEE Standards Documents

IEEE documents are made available for use subject to important notices and legal disclaimers. These notices and disclaimers, or a reference to this page, appear in all standards and may be found under the heading "Important Notice" or "Important Notices and Disclaimers Concerning IEEE Standards Documents."

Notice and Disclaimer of Liability Concerning the Use of IEEE Standards Documents

IEEE Standards documents (standards, recommended practices, and guides), both full-use and trial-use, are developed within IEEE Societies and the Standards Coordinating Committees of the IEEE Standards Association ("IEEE-SA") Standards Board. IEEE ("the Institute") develops its standards through a consensus development process, approved by the American National Standards Institute ("ANSI"), which brings together volunteers representing varied viewpoints and interests to achieve the final product. Volunteers are not necessarily members of the Institute and participate without compensation from IEEE. While IEEE administers the process and establishes rules to promote fairness in the consensus development process, IEEE does not independently evaluate, test, or verify the accuracy of any of the information or the soundness of any judgments contained in its standards.

IEEE does not warrant or represent the accuracy or content of the material contained in its standards, and expressly disclaims all warranties (express, implied and statutory) not included in this or any other document relating to the standard, including, but not limited to, the warranties of: merchantability; fitness for a particular purpose; non-infringement; and quality, accuracy, effectiveness, currency, or completeness of material. In addition, IEEE disclaims any and all conditions relating to: results; and workmanlike effort. IEEE standards documents are supplied "AS IS" and "WITH ALL FAULTS."

Use of an IEEE standard is wholly voluntary. The existence of an IEEE standard does not imply that there are no other ways to produce, test, measure, purchase, market, or provide other goods and services related to the scope of the IEEE standard. Furthermore, the viewpoint expressed at the time a standard is approved and issued is subject to change brought about through developments in the state of the art and comments received from users of the standard.

In publishing and making its standards available, IEEE is not suggesting or rendering professional or other services for, or on behalf of, any person or entity nor is IEEE undertaking to perform any duty owed by any other person or entity to another. Any person utilizing any IEEE Standards document, should rely upon his or her own independent judgment in the exercise of reasonable care in any given circumstances or, as appropriate, seek the advice of a competent professional in determining the appropriateness of a given IEEE standard.

IN NO EVENT SHALL IEEE BE LIABLE FOR ANY DIRECT, INDIRECT, INCIDENTAL, SPECIAL, EXEMPLARY, OR CONSEQUENTIAL DAMAGES (INCLUDING, BUT NOT LIMITED TO: PROCUREMENT OF SUBSTITUTE GOODS OR SERVICES; LOSS OF USE, DATA, OR PROFITS; OR BUSINESS INTERRUPTION) HOWEVER CAUSED AND ON ANY THEORY OF LIABILITY, WHETHER IN CONTRACT, STRICT LIABILITY, OR TORT (INCLUDING NEGLIGENCE OR OTHERWISE) ARISING IN ANY WAY OUT OF THE PUBLICATION, USE OF, OR RELIANCE UPON ANY STANDARD, EVEN IF ADVISED OF THE POSSIBILITY OF SUCH DAMAGE AND REGARDLESS OF WHETHER SUCH DAMAGE WAS FORESEEABLE.

Translations

The IEEE consensus development process involves the review of documents in English only. In the event that an IEEE standard is translated, only the English version published by IEEE should be considered the approved IEEE standard.

Official statements

A statement, written or oral, that is not processed in accordance with the IEEE-SA Standards Board Operations Manual shall not be considered or inferred to be the official position of IEEE or any of its committees and shall not be considered to be, or be relied upon as, a formal position of IEEE. At lectures, symposia, seminars, or educational courses, an individual presenting information on IEEE standards shall make it clear that his or her views should be considered the personal views of that individual rather than the formal position of IEEE.

Comments on standards

Comments for revision of IEEE Standards documents are welcome from any interested party, regardless of membership affiliation with IEEE. However, IEEE does not provide consulting information or advice pertaining to IEEE Standards documents. Suggestions for changes in documents should be in the form of a proposed change of text, together with appropriate supporting comments. Since IEEE standards represent a consensus of concerned interests, it is important that any responses to comments and questions also receive the concurrence of a balance of interests. For this reason, IEEE and the members of its societies and Standards Coordinating Committees are not able to provide an instant response to comments or questions except in those cases where the matter has previously been addressed. For the same reason, IEEE does not respond to interpretation requests. Any person who would like to participate in revisions to an IEEE standard is welcome to join the relevant IEEE working group.

Comments on standards should be submitted to the following address:

Secretary, IEEE-SA Standards Board
445 Hoes Lane
Piscataway, NJ 08854 USA

Laws and regulations

Users of IEEE Standards documents should consult all applicable laws and regulations. Compliance with the provisions of any IEEE Standards document does not imply compliance to any applicable regulatory requirements. Implementers of the standard are responsible for observing or referring to the applicable regulatory requirements. IEEE does not, by the publication of its standards, intend to urge action that is not in compliance with applicable laws, and these documents may not be construed as doing so.

Copyrights

Photocopies

Updating of IEEE Standards documents

Users of IEEE Standards documents should be aware that these documents may be superseded at any time by the issuance of new editions or may be amended from time to time through the issuance of amendments, corrigenda, or errata. An official IEEE document at any point in time consists of the current edition of the document together with any amendments, corrigenda, or errata then in effect.

Every IEEE standard is subjected to review at least every ten years. When a document is more than ten years old and has not undergone a revision process, it is reasonable to conclude that its contents, although still of some value, do not wholly reflect the present state of the art. Users are cautioned to check to determine that they have the latest edition of any IEEE standard.

In order to determine whether a given document is the current edition and whether it has been amended through the issuance of amendments, corrigenda, or errata, visit the IEEE-SA Website at http://ieeexplore.ieee.org/xpl/standards.jsp or contact IEEE at the address listed previously. For more information about the IEEE-SA or IEEE's standards development process, visit the IEEE-SA Website at http://standards.ieee.org.

Errata

Errata, if any, for all IEEE standards can be accessed on the IEEE-SA Website at the following URL: http://standards.ieee.org/findstds/errata/index.html. Users are encouraged to check this URL for errata periodically.

Patents

Attention is called to the possibility that implementation of this standard may require use of subject matter covered by patent rights. By publication of this standard, no position is taken by the IEEE with respect to the existence or validity of any patent rights in connection therewith. If a patent holder or patent applicant has filed a statement of assurance via an Accepted Letter of Assurance, then the statement is listed on the IEEE-SA Website at http://standards.ieee.org/about/sasb/patcom/patents.html. Letters of Assurance may indicate whether the Submitter is willing or unwilling to grant licenses under patent rights without compensation or under reasonable rates, with reasonable terms and conditions that are demonstrably free of any unfair discrimination to applicants desiring to obtain such licenses.

Essential Patent Claims may exist for which a Letter of Assurance has not been received. The IEEE is not responsible for identifying Essential Patent Claims for which a license may be required, for conducting inquiries into the legal validity or scope of Patents Claims, or determining whether any licensing terms or conditions provided in connection with submission of a Letter of Assurance, if any, or in any licensing agreements are reasonable or non-discriminatory. Users of this standard are expressly advised that determination of the validity of any patent rights, and the risk of infringement of such rights, is entirely their own responsibility. Further information may be obtained from the IEEE Standards Association.

Participants

At the time this IEEE guide was completed, the Fault Location Working Group had the following membership:

Joe Mooney, *Chair*
Randall Cunico, *Vice Chair*

Michael Agudo
George Bartok
Gabriel Benmouyal
Brian Boysen
Sukumar Brahma
Patrick T. Carroll
Arvind Chaudhary
Normann Fischer
Fred Friend
Rafael Garcia
Yanfeng Gong
Mansour Jalali
Meyer Kao
Mladen Kezunovic
Ashish Kulshresthra
Tony Napikoski
Damier Novosel
Jim O'Brien
Donald Parker
Simon Richards
Daniel Sabin
Tony Seegers
Steve Turner
Jun Verzosa
Liancheng Wang
Ray Young
Zhiying Zhang
Sergio L. Zimath
Karl Zimmerman

The following members of the individual balloting committee voted on this guide. Balloters may have voted for approval, disapproval, or abstention.

William Ackerman
Ali Al Awazi
George Bartok
Philip Beaumont
Robert Beresh
Wallace Binder
William Bloethe
Brian Boysen
Gustavo Brunello
William Byrd
Paul Cardinal
Arvind Chaudhary
Stephen Conrad
James Cornelison
Luis Coronado
Randall Crellin
Randall Cunico
Alla Deronja
Gary Donner
Gearold O. H. Eidhin
Fred Friend
Rafael Garcia
Frank Gerleve
Jalal Gohari
Stephen Grier
Randall Groves
Ajit Gwal
Keith Harley
Roger Hedding
David Horvath
Yi Hu
Relu Ilie
Brian Johnson
Innocent Kamwa
John Kay
James Kinney
Gary Kobet
Joseph L. Koepfinger
Boris Kogan
Ljubomir Kojovic
Jim Kulchisky
Paneendra KumarBl
Chung-Yiu Lam
Raluca Lascu
Theo Laughner
Michael Lauxman
Roger Lawrence
Albert Livshitz
Federico Lopez
Om P. Malik
Omar Mazzoni
Dean Miller
John Miller
Daleep Mohla
Joe Mooney
Jerry Murphy
R. Jay Murphy
Michael Newman
Gary Nissen
Jim O'Brien
Lorraine Padden
Mirko Palazzo
Donald Parker
Michael Roberts
Charles Rogers
Daniel Sabin
Bartien Sayogo
Thomas Schossig
Tony Seegers
Sepehr Sefidpour
Robert Seitz
Charles Simmons
Veselin Skendzic
Jerry Smith
Gary Smullin
James Swank
Michael Thompson
Demetrios Tziouvaras
Joe Uchiyama
Eric Udren
John Vergis
Jun Verzosa
Ilia Voloh
Liancheng Wang
Kenneth White
James Wilson
Philip Winston
Ray Young
Jian Yu
Luis Zambrano

When the IEEE-SA Standards Board approved this guide on 10 December 2014, it had the following membership:

John Kulick, *Chair*
Jon Walter Rosdahl, *Vice-Chair*
Richard H. Hulett, *Past Chair*
Konstantinos Karachalios, *Secretary*

Peter Balma
Farooq Bari
Ted Burse
Clint Chaplain
Stephen Dukes
Jean-Philippe Faure
Gary Hoffman
Michael Janezic
Jeffrey Katz
Joseph L. Koepfinger*
David Law
Hung Ling
Oleg Logvinov
T. W. Olsen
Glenn Parsons
Ron Peterson
Adrian Stephens
Peter Sutherland
Yatin Trivedi
Phil Winston
Don Wright
Yu Yuan

*Member Emeritus

Also included are the following non-voting IEEE-SA Standards Board liaisons:

Richard DeBlasio, *DOE Representative*
Michael Janezic, *NIST Representative*

Patrick Gibbons
IEEE-SA Content Production and Management

Erin Spiewak
IEEE-SA Technical Program Operations

Introduction

This introduction is not part of IEEE Std C37.114-2014, IEEE Guide for Determining Fault Location on AC Transmission and Distribution Lines.

This guide outlines the techniques and application considerations for determining the location of a fault on ac transmission and distribution lines. The guide reviews traditional approaches and the primary measurement techniques used in modern devices: one- and two-terminal impedance-based methods and traveling-wave methods. Application considerations include: two- and three-terminal lines, series-compensated lines, parallel lines, untransposed lines, underground cables, fault resistance effects, and other power system conditions, including those unique to distribution systems.

Contents

IEEE Guide for Determining Fault Location on AC Transmission and Distribution Lines

1. Overview

1.1 Scope

This guide outlines the techniques and application considerations for determining the location of a fault on ac transmission and distribution lines. This document reviews traditional approaches and the primary measurement techniques used in modern devices: one- and two-terminal impedance-based methods, synchronized sampling methods and traveling-wave methods. Application considerations include: two- and three-terminal lines, series-compensated lines, parallel lines, untransposed lines, tapped lines, underground cables, fault resistance effects, and other power system conditions, including those unique to distribution systems.

1.2 Purpose

The guide assists power system engineers and operators in applying fault-locating techniques on their systems. Users learn the strengths and limitations of fault location data and when further analysis is required using additional methods and when more data must be gathered. This guide assists in fault location and therefore faster restoration of power systems through improved understanding of fault-locating techniques.

1.3 Techniques and requirements for fault-locating devices

This guide discusses various approaches to determine fault location, with emphasis on automatic methods performed by microprocessor devices. The following are some tools used to determine fault location:

- Microprocessor devices
- Short-circuit analysis software
- Customer calls (distribution)
- Line inspection

A device capable of determining the physical fault location has different requirements than a fault detection device:

- The speed to determine fault location is for human users (seconds or minutes), while relays usually need to detect faults within 10 ms to 50 ms. Consequently, additional information and more demanding and slower numerical techniques become available.
- A best fault data window can be selected to reduce errors.
- Communications enable transmitting data to a remote site using dedicated data communications or supervisory control and data acquisition (SCADA).
- More accurate phasor calculation*s* can be achieved by using digital filtering of the voltage and current samples that would introduce an unacceptable delay for the relaying applications.
- High accuracy is needed for efficient dispatch of repair crews. Unlike protective relays, which need to detect whether faults are in the zones established by current transformer locations, pilot channels, and reach coordination, fault location data must be very accurate to save the time and reduce the expenses of the crews searching in bad weather and/or over rough terrain.

In this guide, the following are examined:

- Data and equipment required
- Commonly used algorithms
- Accuracy limitations of one-ended and two-ended impedance-based fault location methods
- Synchronized sampling method
- Traveling-wave methods and other methods
- Issues regarding distribution systems and underground cables

1.4 How to determine line parameters

1.4.1 Line parameters for impedance estimation

Accurate fault location based upon impedance estimation will depend on the accuracy of calculated transmission impedances. The common method of calculation is based on equations developed by J. R. Carson, and published in 1926 [B3][1]. There are many good textbooks devoted to the topic of power system

[1] The numbers in brackets correspond to those of the bibliography in Annex A.

analysis that will show the development of Carson's equations used for determining the line impedances. It is not necessary to show the development of these equations here. Relay engineers have used the equations for many years to model power systems for performing short-circuit studies. A typical short-circuit computer program would utilize short or medium length line impedances derived from calculations based upon the assumption of fully transposed lines over a homogeneous right-of-way. The only significant details added to the model are the effects of zero-sequence mutual coupling between parallel sections of lines. The results obtained from these impedance models for determining relay coordination and performing postmortem analysis are very good. The question that remains is whether these calculated impedances are sufficient to obtain the desired level of accuracy in the location of faults. Accuracy to within 1% of error has been claimed for the calculated impedances (Eriksson, Saha, and Rockfeller [B5]).

Another method of determining the line impedance parameters involves the direct measurement of the open circuit, and short-circuit voltages and currents. The accuracy is about the same as calculations based on Carson's equations. This method requires special equipment and network conditions (i.e., the line must be taken out of service) to set up the tests.

A third method involves the estimation of the line parameters through the solution of two-port equations based on synchronized phasor measurement obtained from direct measurements from a digital relay or a fault recorder. The use of controlled tests to obtain the data and using the higher sampling rate of a digital recorder can result in impedance parameters with a high accuracy. It should be noted that all three techniques rely on an accurate value for the length of the line.

It is suggested that the calculations for most lines can still be made using Carson's equations. These parameters can then be verified using synchronized phasors of method three or by experience from the calculation of the locations from faults with verifiable locations. In spite of the accuracy of the line impedance parameters, the accuracy of fault location will be dependent upon the location technique employed, the sampling rate of the data collected, and the presence of unknown variables, most notably the amount of fault resistance.

Line parameter errors introduced on lines without transpositions are described in 5.12.

1.4.2 Parameters required for traveling-wave fault locating

When a current-based traveling-wave fault locator is commissioned, the remote units are programmed with the substation and line name, sensitivity, and default sampling settings. No specific line parameters (impedances, etc.) are required for the remote units. The host personal computer (PC), on command, can receive the data from each of the remote units. Once the PC has the data files, the information is analyzed and the line length can be determined. The only inputs required to analyze fault data with the traveling-wave fault locator are line length and wave velocity. The individual line length can be determined by energizing the line. The procedure is to energize the line in a radial fashion and then measure the time the reflected wave takes to return to the source. The known line length is compared with the length determined by the timing of the reflected wave. This method may not always give accurate results due to the effects of pre-insertion resistors and the closing point on the voltage sine wave. It is not always necessary to rely solely on this method because the line length calibration can also be determined from evaluation of any faults occurring on adjacent line sections.

2. Definitions, acronyms, and abbreviations

2.1 Definitions

For the purposes of this document, the following terms and definitions apply. The *IEEE Standards Dictionary Online* should be consulted for terms not defined in this clause.[2]

dc thumping: A procedure of applying dc voltage pulses to an underground cable with the intent of locating a cable irregularity with a listening device.

digital recorder: A device that can perform analog-to-digital conversions and store the information in digital form for later retrieval.

distributed intelligence: Gathering data from many different devices for analysis and decision making in a central device.

evolving fault: A fault where the phases involved change over time. For example, a phase-to-ground fault becomes a phase-to-phase-to-ground fault.

fault location error: Percentage error in fault location estimate based on the total line length: e (error) = (instrument reading – exact distance to the fault) / total line length.

homogeneous line: A transmission line where impedance is distributed uniformly on the whole length.

homogeneous system: A transmission system where the local and remote source sequence impedances have the same system angle as the line sequence impedance.

intelligent electronic device (IED): Any device incorporating one or more processors with the capability to receive or send data/control from or to an external source (e.g., electronic multifunction meters, digital relays, controllers).

nomograph: A graph that plots measured fault location versus actual fault location by compensating for known system errors.

Peterson's coil: A tunable reactor used for impedance grounding a distribution or transmission system that is usually tuned to be in resonance with the capacitance to ground of all system components.

pre-insertion resistor: A resistor that is inserted in parallel with each set of breaker contacts during the closing stroke of the breaker.

series-compensated line: A transmission line with series capacitors.

superposition current: The summation current at any point in a linear network that results from the voltages applied at various points in the network.

synchronized phasor or **synchrophasor:** A phasor calculated from data samples using a standard time signal as the reference for the measurement.

time code stamping: Associating an accurate time with a particular event.

[2] *IEEE Standards Dictionary Online* subscription is available at: http://www.ieee.org/portal/innovate/products/standard/standards_dictionary.html.

time synchronization: A method of using a time signal from an accurate time source for time-synchronizing equipment.

traveling wave: The resulting wave when the electric variation in a circuit takes the form of translation of energy along a conductor, such energy being always equally divided between current and potential forms.

2.2 Acronyms and abbreviations

MOV	metal oxide varistors
PMU	phasor measurement units
SCADA	supervisory control and data acquisition
SLG	single-line to ground

3. One-ended impedance-based measurement techniques

3.1 Background

One-ended impedance-based fault locators calculate the fault location from the apparent impedance seen looking into the line from one end. To locate all fault types, the phase-to-ground voltages and currents in each phase must be measured. (If only line-to-line voltages are available, it is possible to locate phase-to-phase faults, and additionally, if the zero-sequence source impedance, Z_0, is known, the location for phase-to-ground faults can also be estimated).

If the fault resistance is assumed to be zero, use one of the impedance calculations in Table 1 to estimate fault location. The exact mathematical equations for fault location taking into account fault resistance and load are found in 3.3.

Table 1—Simple impedance equations

Fault type	Positive-sequence impedance equation (mZ_{1L} =)
a–ground	$V_a / (I_a + kI_R)$
b–ground	$V_b / (I_b + kI_R)$
c–ground	$V_c / (I_c + kI_R)$
a–b or a–b–g	V_{ab} / I_{ab}
b–c or b–c–g	V_{bc} / I_{bc}
c–a or c–a–g	V_{ca} / I_{ca}
a–b–c	Any of the following: V_{ab} / I_{ab}, V_{bc} / I_{bc}, V_{ca} / I_{ca}

where

k	is $(Z_{0L} - Z_{1L}) / 3Z_{1L}$
Z_{0L}	is the zero-sequence line impedance
m	is the per unit distance to fault (e.g., distance to fault in kilometers divided by the total line length in kilometers)
I_R	is the residual current

Voltage and current data are used to determine the impedance to the fault location, as shown in Table 1. By knowing the line impedance per unit, the distance to the fault per unit can be determined. A correct fault location estimate, unfortunately, is affected by many factors not represented by these equations:

a) The combined effect of the load current and fault resistance (reactance effect). The value of the fault resistance may be particularly high for ground faults, which represent the majority of the faults on overhead lines.

b) Inaccurate fault type (faulted phases) identification.

c) Influence of zero-sequence mutual effects.

d) Uncertainty about the line parameters, particularly zero-sequence impedance. It is often difficult to obtain an accurate zero-sequence impedance (Z_{0L}) for the line. The value of Z_{0L} is affected by soil resistivity, which can be difficult to measure and may be changeable. A 20% error in Z_{0L} can introduce a 15% error in the calculated fault location. In addition, this impedance is not uniformly distributed along the line length. (100 to 1 variation in earth resistivity produces about a 2 to 1 change in Z_0.)

e) Insufficient accuracy of the line model (e.g., untransposed lines are represented as being transposed, and charging capacitance is not considered).

f) Presence of shunt reactors and capacitors.

g) Load flow unbalance.

h) Series-compensated and multi-terminal lines.

i) Measurement errors, current and voltage transformer errors, and bit resolution of analog to digital conversion (A/D) system.

j) The filtering system necessary to extract the phase voltages and current phasors. For example, if the fault voltages and currents do not reach steady-state value (as in a fault with time varying resistance) or if the fault is cleared with a delay smaller than the filter nominal response time, then the estimated fault location could have substantial errors.

k) Clock sampling rate of the device.

To improve the fault location estimate, it is important to eliminate or reduce errors caused by inadequate assumptions or inaccurate data applied to fault location algorithms. The algorithms will be more accurate if more information about the system is available.

3.2 Implementation: data and equipment required

One-ended fault location methods require the following equipment for implementation:

— A microprocessor-based relay or other device that measures three-phase voltages and currents and calculates a fault location estimate

— A communications interface to remotely obtain the fault location estimate

The following data or information is required from the equipment:

— Phase-to-ground voltages and phase currents. Some algorithms can accommodate delta-connected voltages, but only if zero-sequence source impedance is known at the time of fault (Schweitzer [B55]).

— Correct fault type must be known (e.g., a-g, b-g, c-g, a-b).

— Some methods require pre-fault load data.

3.3 Determination of measurement error

3.3.1 Background

There are different methods for determining the measured fault location error. Following are three methods for determining the measurement error that will be described further, including their advantages and the intended use for each method:

a) Absolute error

b) Relative error based on line length

c) Traditional relative error

While absolute error gives a value regardless of the line length, relative errors are more useful to compare various fault location methodologies independently of the power system. For example, for a 10-mile short line, a calculation error of 5 miles is large. For a 200-mile-long line, a calculation error of 5 miles is relatively small.

3.3.2 Absolute error

Absolute error is defined as:

$$e_a = \left| m_m - m_t \right| \tag{1}$$

where

e_a is the absolute error – per unit (p.u.), percentage (%), or distance (miles or kilometers)

m_m is the measured fault location – per unit (p.u.), percentage (%), or distance (miles or kilometers)

m_t is the true fault location – per unit (p.u.), percentage (%), or distance (miles or kilometers)

Understanding a range of error values, for a particular fault location methodology used in a particular power system, could provide useful guidance to the crew that needs to travel to an actual location of the fault to fix a problem.

3.3.3 Relative error based on line length

The fault location error based on line length is calculated as follows:

$$e_l = \frac{\left| m_m - m_t \right|}{L} \tag{2}$$

where

e_l is the relative error based on line length – per unit (p.u.), percentage (%), or distance (miles or kilometers)

L is the line length – per unit (p.u.), percentage (%), or distance (miles or kilometers)

3.3.4 Traditional relative error

The traditional fault location error is calculated as follows:

$$e_t = \frac{|m_m - m_t|}{m_t} \tag{3}$$

where

e_t is the traditional relative error – per unit (p.u.) or percentage (%)

Unless this relative error is used within the context of pure statistical analysis, it is less intuitive to practical application in locating faults.

3.3.5 Comparison of measurement error methods

The advantage of the definition based on line length is that the absolute fault location error is independent of the location of the fault. For example, for a 100-mile-long line with an error of 5 miles, the error e_l is 0.05 p.u. or 5% regardless if the fault is at the beginning of the line or at the end of the line.

For the traditional method, the same absolute error of 5 miles for the same line 100-mile line would be different depending on the fault location. For example if a fault is at 10 miles from the substation at the beginning of the line, the error e_t is 0.5 p.u. or 50%. If fault is at 90 miles from the substation at beginning of the line (or 10 miles from the substation at the other end of the line), the error e_t is 0.056 p.u. or 5.56%.

For single-ended algorithms, both methods could be used. However, for double-ended methods, it could be confusing to use the traditional method, as the fault location could be calculated from both ends of the line, so the true value needs a common reference to be compared with.

Furthermore, as for a particular power network, the combination of system source impedance ratios and location of the fault have a major effect on accuracy of single-ended algorithms. When evaluating and comparing errors of various algorithms, it is very important to take this into account. It may be easier to compare various algorithms having a common reference (such as the line length). Staging faults at the end of the line with favorable source impedance ratios could result in a misleading high accuracy.

From a statistical standpoint, the interest is in the deviation of the predicted location from the true location based on the total (i.e., total line length). Each line is treated as the total distribution of all possible faults and each fault would be treated as a single sample of this distribution. The absolute error stated here is actually a sample error. For the purposes of fault location, it is preferred then to state the relative error based on the line length. Using this preferred method, the errors for several faults on a given line would appear uniform regardless of their location along the line.

The reverse of this would be to apply a predicted error (based on experience) to a measured location to assist in a line patrol. For example, a fault is predicted to be of 23 miles on a 100-mile line. From experience, it could be predicted that the true location will be discovered within 5% of the line length. Therefore, a patrol would be instructed to expect the location to be somewhere between 18 and 28 miles from the substation.

3.4 Error due to reactance effect

Issues in estimating the fault location using local data can be described by considering the simplified, single-line diagram of the system shown in Figure 1.

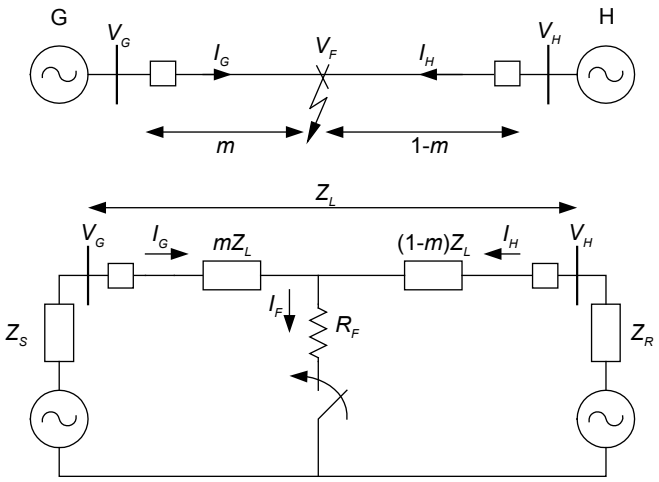

Figure 1—One line and equivalent circuit for a three-phase fault on a transmission line with two sources, G and H

A fault with resistance R_F is on the homogeneous line with an impedance Z_L between terminals G and H. The terminal voltages are V_G and V_H. The currents from both ends of the line, I_G and I_H, contribute to the total current in the fault, I_F. The parts of the system behind the local and remote terminals are replaced with the Thevenin equivalents having the impedances Z_S and Z_R (source impedances). The voltage drop from terminal G can be written easily along with the per unit fault location, m:

$$V_G = mZ_L I_G + R_F I_F \tag{4}$$

where

V_G is the voltage at terminal G

m is the distance to the fault in per unit

Z_L is the line impedance between terminals G and H

I_G is the line current from terminal G

R_F is the fault resistance

I_F is the total fault current

The value of the impedance measured at terminal G may be found by dividing Equation (4) by the measured current, I_G.

$$Z_{FG} = \frac{V_G}{I_G} = mZ_L + R_F \frac{I_F}{I_G} \tag{5}$$

where

Z_{FG} is the apparent impedance to the fault measured at terminal G

If the ratio of the fault current, I_F, and the current at the fault locator location, I_G, is a complex number, the fault resistance will be represented as an impedance with a reactive component. The reactive component can be inductive or capacitive, depending on the angle of the ratio of the two currents. The reactive component will be zero only if the angle is zero. This is the case if the infeed current from the remote

terminal, I_H, is zero or is in phase with the local current, I_G. The reactive component can produce an error in the fault location estimate as shown in Figure 2.

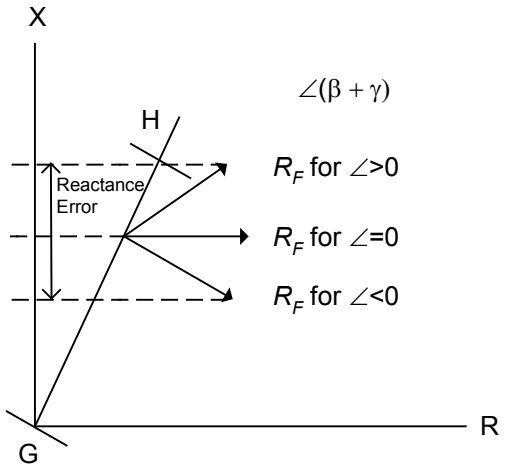

Figure 2—Graphical interpretation of the fault resistance and pre-fault load errors

In order to analyze which parameters affect the angle of I_F/I_G, superposition may be used to separate the pre-fault and fault systems. Let the pre-fault load current be represented by I_L, and the difference (superimposed) current by $\Delta I_G = I_G - I_L$. Equation (5) may be rewritten as:

$$Z_{FG} = \frac{V_G}{I_G} = mZ_L + R_F \frac{1}{d_S n_S} \tag{6}$$

where

d_S is the current distribution factor as shown in Equation (7)

n_S is the circuit loading factor as shown in Equation (8)

$$d_S = \frac{\Delta I_G}{I_F} = \frac{Z_H + (1-m)Z_L}{Z_H + Z_L + Z_G} = |d_S| \angle \beta \tag{7}$$

$$n_S = \frac{I_G}{I_G - I_L} = \frac{I_G}{\Delta I_G} = |n_S| \angle \gamma \tag{8}$$

Thus the angle of the current ratio I_F/I_G, and therefore the reactive component caused by the fault resistance, is determined by two factors. The current distribution factor, d_S is determined by the system impedances. If the system is homogeneous, then the angle of d_S, β, is zero. If there is load flow on the system, the angle of n_S, γ, will not be zero. However, if the magnitude of the fault current, I_G, is much greater than the magnitude of the load current, I_L, the angle γ will approach zero. The sum of the angles, $(\beta + \gamma)$, will determine the reactive component caused by fault resistance, R_F.

Various techniques can be used to reduce the effect of the fault resistance, R_F, most of which need to make certain simplifying assumptions to achieve implementation. The performance of the fault location algorithm, with respect to R_F, is dependent on the assumptions that have been made. Some typical algorithms are described in 3.5.

3.5 Algorithms

3.5.1 Background

Depending on the circuit data available, different fault location algorithms may be implemented. This section provides an overview of different fault location algorithms that attempt to limit the error due to fault resistance and load current.

3.5.1 Simple reactance method

With the simple reactance method, the device measures the apparent impedance, then determines the ratio of the measured reactance to the reactance of the entire line. This ratio is proportional to the distance to the fault. The method assumes that the current through the fault resistance is in phase with the current at the measurement point, and there is no load prior to the fault.

The reactance algorithm is one of the earliest algorithms that compensates for the fault resistance by measuring only the imaginary part of the apparent line impedance Z_G. Per unit distance to the fault is shown in Equation (9):

$$m = \frac{Im(V_G / I_G)}{Im(Z_L)} \tag{9}$$

For the line-to-ground fault (a-g), the calculation would be as shown in Equation (10):

$$m = Im\left[\frac{V_{Ga}}{I_{Ga} + k_0 I_R)}\right] \Big/ Im(Z_{1L}) \tag{10}$$

where

k_0 is $(Z_{0L} - Z_{1L})/3Z_{1L}$ and residual current $I_R = 3I_0$.

The error is zero if the fault resistance is zero or if I_G and I_F are in phase. For a fault with a high resistance, the algorithm may introduce considerable reactance error, as shown in Figure 2. The reactance effect increases or reduces the apparent line reactance to the fault, leading to an error in apparent fault location. Some one-terminal data algorithms, described in 3.5.2, have been developed to compensate for the reactance effect.

3.5.2 Fault location method without using source impedances

The above can be improved upon with elimination of load current by determining the change in current on occurrence of a fault. This method, which uses superposition current ΔI_G, has been discussed in the literature by various researchers, most notably by Takagi, et al [B58]. In addition, Eriksson, Saha, and

Rockfeller [B5] use the distribution factor, d_S, to represent the voltage drop across the fault resistance, R_F. Equation (4) can be written as:

$$V_G = mZ_{1L}I_G + R_F \frac{\Delta I_G}{d_S} \tag{11}$$

Equation (12) shows the result that is obtained if both sides of Equation (11) are multiplied by the complex conjugate, ΔI_G^*, using only the imaginary part:

$$Im\left(V_G \Delta I_G^*\right) = mIm\left(Z_L I_G \Delta I_G^*\right) + R_F Im\left(\frac{1}{d_S}\right) \tag{12}$$

If the system is homogenous, the angle of the current distribution factor is nearly zero ($Im(1/d_S) = 0$) and the fault location is:

$$m = \frac{Im\left(V_G \Delta I_G^*\right)}{Im\left(Z_L I_G \Delta I_G^*\right)} \tag{13}$$

The current distribution factors for the parts of the network, located on either side of the fault point, are assumed to have the same arguments (consequently, $\beta = 0$). Put another way, this method is accurate if the fault current at the fault locator is in phase with the fault current at the fault. The error of the method is proportional to the fault resistance and sin β (see Figure 2). The value of β generally varies with the distance to fault and cannot be calculated unless the source impedances are accurately known. In general, the stronger the local source, the closer the value of β tends toward 0. This method compensates for the error caused by the circuit loading (complex number n_S, angle γ).

A method in Novosel, et al. [B39] uses an assumption that the current distribution factor in the negative-sequence network is a real number. For the unbalanced ground faults, this method does not require pre-fault currents, and the zero-sequence distribution factor does not affect the fault location estimate. Although adequate accuracy is expected for the variety of fault cases, the assumptions above may lead to approximate solutions. The methods in this category compensate for load and fault resistance but are sensitive to an argument of the current distribution factor that is not equal to zero in nonhomogenous systems. One implementation of this multiplies both the numerator and denominator of Equation (13) by a phasor of unity magnitude and angle β.

Another method (modified Takagi) uses the zero-sequence current (I_R) instead of the superposition current (ΔI_G), and angle correction (β) derived from the source impedance data to account for a nonhomogeneous system:

$$m = \frac{Im\left(V_G I_R^* e^{-j\beta}\right)}{Im\left(Z_{1L} I_G I_R^* e^{-j\beta}\right)} \tag{14}$$

This method can improve the fault location estimate by reducing the reactance effect error. However, angle correction, β, makes the fault location accurate at only one point on the line. The result is that ground faults at other points on the line do not have a precise β setting to achieve accurate fault location.

3.5.3 Fault location methods using source impedance

The significance of the distribution factor is discounted in the method described in Eriksson, Saha, and Rockfeller, [B5], which uses a positive-sequence model of the transmission line and source impedances at

the two ends of the line. In this case, knowledge of the source impedances is required, which is not necessarily always known to the desired accuracy.

If the source impedances are known, the fault location can be accurately estimated without assumptions. One method discussed in Eriksson, Saha, and Rockfeller [B5] substitutes Equation (7) in Equation (11). Since the current distribution factor d_S is a function of the source impedances, the line impedance, and the unknown fault location m, a quadratic equation follows:

$$m^2 - mk_1 + k_2 - k_3 R_F = 0 \tag{15}$$

where

k_1 complex function of local voltage

k_2 complex function of current

k_3 complex function of source impedances

By separating Equation (15) into a real and an imaginary part, one has two equations with two unknowns, m and R_F. The per unit distance to the fault m can be calculated by eliminating R_F and solving for m.

Methods using source impedances are not sensitive to the reactance effect (compensation for load and fault resistance, and argument of current distribution factor) but require the input of the source impedances as the setting parameters. They provide very accurate results for every network if the source impedances are equal to the set value. Errors can occur when the source impedances are not equal to the set values used by the fault locator.

4. Two-terminal data methods

4.1 Background

Present communications technology allows for use of data from both ends of the transmission line. The calculation of fault location using data from two ends is fundamentally similar to the single-ended methods except now a means exists to determine and reduce or eliminate the effect of fault resistance and other similar factors that tend to throw off the accuracy of the estimate. These factors, such as nontranspositions, strong or weak sources, loading, and others, have been discussed earlier. There have been many articles on variations of the fundamental techniques aimed at improving the accuracy in locating faults. Details of many of these variations can be found in the articles referenced in this guide (i.e., Girgis, Hart, and Peterson [B10], Hart, Novosel, and Udren [B15], Kezunovic [B24], Lawrence, Cabeza, and Hochberg [B31], Novosel, et al. [B38], and Tziouvaras, Roberts, and Benmouya [B61].

Positive, negative, or zero sequence components may be used and the choice depends on the type of fault and on the extent of system imbalances such as mutual coupling (Makki, et al. [B35]). Positive-sequence components are present in all fault types which simplifies automation because the fault type does not need to be calculated. Negative-sequence components are useful for mitigating the effects of mutual coupling and are present in most fault types except for balanced three-phase faults (Turner [B60]). Zero-sequence components are also useful especially when system imbalances are properly mitigated but are only present in unbalanced fault types. The main drawback is the fact that data from both ends must be gathered at one location to be analyzed, whereas the one-terminal location can be done at the line terminal by the relay or other device collecting the data. Effective two-terminal fault location requires an efficient means of collecting oscillographic or phasor data from electronic devices at each end of a line following a fault and processing that data automatically. To simplify the procedure of providing the utility personnel with the

proper information at the proper location (such as dispatching center) when needed, the system-wide solution is desirable (Girgis, Hart, and Peterson [B10]).

This location technique, therefore, takes more time, but speed is not critical for human users. A response in seconds or minutes is adequate. The collected data must also be at least roughly synchronized from each end before analysis is performed. This can be accomplished analytically or through time code stamping. Factors incorporated in the calculations to handle specific error-causing problems may further complicate analysis. Software or other analysis tools are required to properly identify parameters for the fault and implement a two-terminal algorithm. The two-terminal technique has been tested in the field with accurate results (Novosel, et al. [B38], Peterson, et al. [B44]).

An emerging fault location approach that uses two- or multiple-ended data measurement is based on the use of synchronized samples (not phasors). This time domain technique is extremely accurate irrespective of the fault resistance and has advantages when used with high-speed breakers since it can perform calculations within the first ½-cycle and before the opening of the breaker removes access to the measured signals. This technique has been applied to actual data from several types of transmission line configurations and yielded very accurate results (Gopalakrishnan, et al. [B14], Kezunovic and Perunicic [B29], Kezunovic, Perunicic, and Mrkic [B30], Luo, Kezunovic, and Sevick [B34], Phadke, et al. [B45]).

4.2 Implementation requirements

Two-terminal fault location methods require the following equipment for implementation:

- A microprocessor-based relay or other intelligent electronic device (IED) that measures three-phase voltages and currents at each end with time code stamp.
- Modems and other communications equipment to transfer data to a central site or to the other end of the line.
- Technical personnel or computer equipment at central site for collecting data, performing analysis, and calculating fault location estimate. This may include hardware or software aids.
- Remote communications.

The following data or information is required from the equipment:

- Phase-to-ground voltages and phase currents
- Correlation of time stamps or targeting information within reasonable accuracy to perform phasor calculations on data from both ends

Software tools enable fault location computation at the level needed by the user (Peterson, et al. [B44]). The tool produces a single value for a location of the fault and a report in a short time after fault occurrence. All fault data are then archived for statistical analysis allowing an improved management of the electrical system. Complexity of the system is hidden to the user considering both generation and analysis of transient data through use of advanced data-processing tools. Fault data are processed and analyzed in automated mode and the time required by station engineers for evaluation of each fault is strongly reduced. By using modern data-analysis tools and receiving fault location information when required, the utility personnel can, with much more ease, analyze the status of the electrical power system and reduce duration and number of outages.

Furthermore, Internet and web-based communication technologies open new possibilities for an enhanced handling of fault data for fault location estimation. Distributed server-client applications may be used to achieve cost-effective and flexible access to fault data. As one of the examples, web-based computing

technology can be applied to access and analyze fault data and calculate fault location simply using the web browser software on a client PC connected to the Internet. No additional software is needed on this PC.

4.3 System parameters

The system represented in Figure 3 can be used to illustrate the approach used in locating faults based upon information gathered from two terminals.

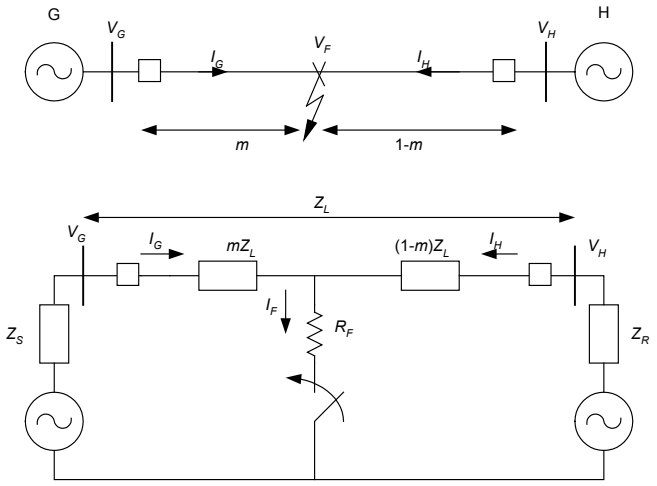

Figure 3—One-line and equivalent circuit for a fault on a transmission line with two sources

4.4 Algorithms

4.4.1 Background

Two-terminal fault location techniques are usually based on the following approach. As shown in Figure 3, the fault is at location *m* (per unit) of the line from bus G and (1–*m*) (per unit) from bus H. The voltage at the fault is denoted as V_F, and the bus voltages and currents are as indicated in the figure. Use of voltage/current relationships in all three phases *a*, *b*, and *c* yields the results found in Equation (16) and Equation (17):

$$\left(V_{GF}\right)_{abc} = mZ_{Labc}\left(I_{GF}\right)_{abc} + V_F \tag{16}$$

$$\left(V_{HF}\right)_{abc} = \left(1-m\right)Z_{Labc}\left(I_{HF}\right)_{abc} + V_F \tag{17}$$

Subtracting the two equations to eliminate the unknown V_F results in Equation (18):

$$\left(V_{GF}\right)_{abc} - \left(V_{HF}\right)_{abc} = mZ_{Labc}\left(I_{GF}\right)_{abc} + \left(m-1\right)Z_{Labc}\left(I_{HF}\right)_{abc} \tag{18}$$

This equation can be solved for the real *m*, and the phase values can be substituted with the symmetrical components.

4.4.2 Synchronized versus un-synchronized phasors for fault location

Consider the example where the fault location is performed on a two-terminal transmission line using the negative sequence network as shown in Figure 4.

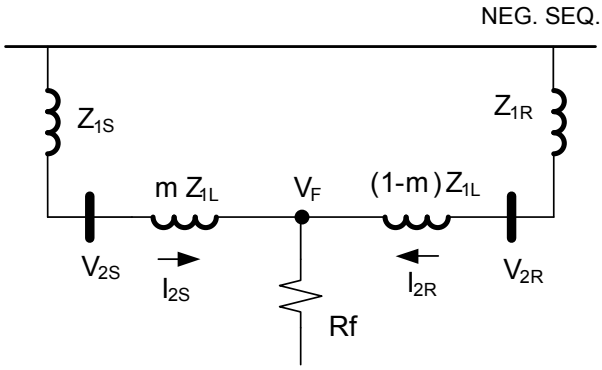

Figure 4—Negative sequence network

In Figure 4, Z_{1L} is the line positive sequence impedance and Rf is fault resistance. V_{2S} and I_{2S} are the negative sequence voltage and current phasors measured at the left substation and V_{2R} and I_{2R} are the negative sequence voltage and current phasors measured at the right substation.

Equation (19) is at the fault point where *m* is a scalar and all other variables are phasors:

$$V_{2S} - m \times Z_{1L} \times I_{2S} = V_{2R} - (1-m) \times Z_{1L} \times I_{2R} \tag{19}$$

From Equation (19), the per unit distance *m* to the fault from the left bus can be computed as:

$$m = \frac{V_{2S} - V_{2R} + Z_{1L} \times I_{2R}}{Z_{1L} \times (I_{2S} + I_{2R})} \tag{20}$$

Equation (20) assumes that the phasors on the left and right sides of the line are synchronized. If this is not the case, in order to obtain an error-free fault location, the left-hand side phasors have to be rotated by an angle corresponding to the synchronizing error t_{Δ}. Equation (20) becomes then:

$$m = \frac{V_{2S} \times e^{2\pi f \times t_{\Delta}} - V_{2R} + Z_{1L} \times I_{2R}}{Z_{1L} \times (I_{2S} \times e^{2\pi f \times t_{\Delta}} + I_{2R})} \tag{21}$$

Equation (20) can be expressed under a different form:

$$V_{2S} - m \times Z_{1L} \times I_{2S} = \left(\frac{V_{2R}}{I_{2R}} - (1-m) \times Z_{1L} \right) \times I_{2R} \tag{22}$$

Introducing the compensation angle to take into account the error in synchronizing, obtains:

$$V_{2S} - m \times Z_{1L} \times I_{2S} = \left(\frac{V_{2R} \times e^{2\pi f \times t_{\Delta}}}{I_{2R} \times e^{2\pi f \times t_{\Delta}}} - (1-m) \times Z_{1L} \right) \times I_{2R} \times e^{2\pi f \times t_{\Delta}} \tag{23}$$

Equation (23) can be otherwise expressed as:

$$\frac{V_{2S} - m \times Z_{1L} \times I_{2S}}{\frac{V_{2R}}{I_{2R}} - (1-m) \times Z_{1L}} = I_{2R} \times e^{2\pi f \times t_{\Delta}} \tag{24}$$

Equating the magnitudes on the left-hand and right-hand sides of Equation (24):

$$\frac{\left|V_{2S} - m \times Z_{1L} \times I_{2S}\right|}{\left|\frac{V_{2R}}{I_{2R}} - (1-m) \times Z_{1L}\right|} = \left|I_{2R} \times e^{2\pi f \times t_{\Delta}}\right| \tag{25}$$

Introducing the next identity:

$$\left|I_{2R} \times e^{2\pi f \times t_{\Delta}}\right| = \left|I_{2R}\right| \tag{26}$$

Equation (25) simply becomes:

$$\frac{\left|V_{2S} - m \times Z_{1L} \times I_{2S}\right|}{\left|\frac{V_{2R}}{I_{2R}} - (1-m) \times Z_{1L}\right|} = \left|I_{2R}\right| \tag{27}$$

By solving Equation (27) for the distance *m*, the result is a quadratic equation (Tziouvaras, Roberts, and Benmouyal [B61]):

$$A \times m^2 + B \times m + C = 0 \tag{28}$$

In Equation (28), *A*, *B*, and *C* are functions of the real and imaginary parts of V_{2S}, I_{2S}, V_{2R}, I_{2R}, and Z_{1L}. The root of the quadratic equation that lies between 0 and 1 is the solution to the fault location.

Equation (27) leads to a remarkable result and that is the compensating angle to take into account the synchronization error has simply vanished. One may conclude that the application for fault location of Equation (9) can be done with un-synchronized phasors. This will be true only under the condition that the voltages and currents during the fault have reached a steady state, i.e., constant magnitude and constant phase angle. This additional subtlety relates to the fault resistance shown as Rf in Figure 4 and can be explained as follows:

— If the fault resistance Rf is constant, the phasors V_{2S}, I_{2S}, V_{2R}, and I_{2R} will reach a constant magnitude and phase angle in the fault steady state. Because of this, the negative sequence phasors on the left and right sides do not have to be measured at the same instant but could be measured with a time interval between the measurements. Even if the phasors are not synchronously measured, Equation (27) will still provide the proper fault location.

— If the fault resistance Rf is not constant but time-varying, for each different value of Rf, the V_{2S}, I_{2S}, V_{2R}, and I_{2R} the phasors will have different magnitudes and phase angles. In order to be able to apply Equation (27), it is necessary to measure all four phasors at the same instant to correspond to a single value of the fault resistance Rf, which means that the four phasors have to be synchronously acquired (Turner [B60]). If this is not the case, errors will be introduced in the fault location.

As an example of the impact of the error in synchronization on two-ended fault location, consider the case of a phase A-to-ground fault on a 230-kV transmission line at a distance equal to 0.62 p.u. from the left substation. Referring to Figure 4, the following values are recorded after the fault has reached steady state:

$$\begin{aligned} Z_{1L} &= 1.3951 + j19.9513\Omega \\ V_{2S} &= -7642.4 - j591.43V \\ I_{2S} &= 144.94 - j1526.2A \\ V_{2R} &= -15172 + j80.335V \\ I_{2R} &= 255.55 - j1495.6A \end{aligned} \tag{29}$$

After the fault has reached steady state, Figure 5 provides the plot of the distance to the fault using Equation (21) and Equations (27) and (28) as a function in the error in synchronization. As expected, the solution based on Equation (27) is immune to any synchronizing error.

Figure 6 shows the distance to the fault percentage error as a function of the synchronizing error when the solution based on Equation (21) is used.

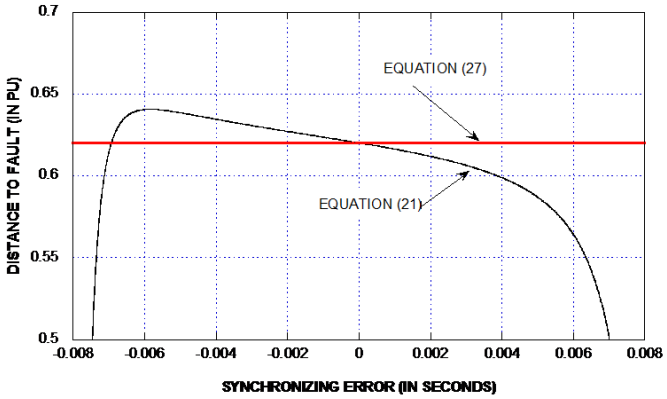

Figure 5—Distance to fault as a function of synchronizing error using Equation (21) and Equation (27)

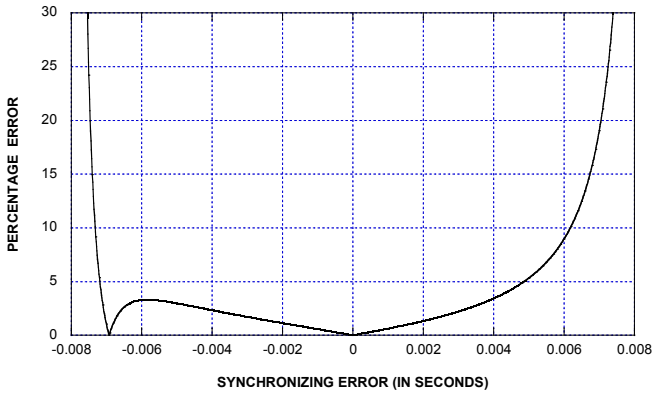

Figure 6—Error in fault location as a function of the synchronizing error using Equation (21)

These considerations developed in this paragraph imply that it is better to acquire phasors synchronously when applying fault location on two or more than two terminals. Subclauses 4.4.3.1 and 4.4.3.2 describe how this can be achieved.

4.4.3 Acquiring phasors synchronously

4.4.3.1 Use of synchrophasors in fault location

Synchrophasors are defined by IEEE Std C37.118.1™-2011 [B20], IEEE Std C37.118a™-2104 [B21], and IEEE Std C37.118.2™-2011 [B22].

Phasors originating from two locations of a network with the same timestamp are expected to be synchronized. Synchrophasors are typically created by processing instantaneous samples of a voltage or current waveform through a filtering system that will provide the magnitude and phase angle of the waveform in the form of rectangular or polar coordinates. Synchrophasors are processed in devices located at the substations and called phasor measurement units (PMUs). These PMUs could be dedicated devices to the sole measurement of synchrophasors or protective relays or digital fault recorders with an imbedded synchrophasor function.

Synchrophasors can be used for the purpose of fault locating using Equation (20) by deriving the negative sequence voltage and current phasors from synchrophasors bearing the same timestamp. When using synchrophasors for the purpose of fault location with two or more terminals, the following items should be considered:

- The nature of the filtering system implemented in the different PMUs
- The acquisition rate of the synchrophasors from the different PMUs
- The data window used in the synchrophasors filtering system

If the synchrophasor filtering system is not the same at all terminals, the transient response of the synchrophasors at different locations will be different and errors can be introduced in the fault location during the interval of time before the fault reaches its steady-state value.

Most important is the acquisition rate of the synchrophasors. As an example, an acquisition rate of 60 measurements per second (or 1 measurement per cycle) will lead to a poorly defined fault location.

A longer synchrophasor filtering data window will result in a less accurate fault location. For example, a data window of four to five cycles may not allow phasor measurement to complete before the fault has been cleared.

4.4.3.2 Use of synchronized sampling in fault location

Synchronized sampling can be used in two or multi-terminal fault locating when voltage and current instantaneous samples are referenced by individual timestamps to the same time reference. Universal Time Coordinated is the most commonly used time reference on power network applications.

Synchronized samples can be generated by disturbance recorders or protective relays and can be distributed or transported in the form of a proprietary event report format or a standard COMTRADE file.

The main differences between using synchrophasors or synchronizing sampling for fault location are the following:

— When using synchronized sampling, applying the same filtering system at all terminals results in the same transient response of the filters for all computed phasors. This will be a definite advantage if the fault location has to be performed before the fault reaches a steady state condition.

— When using synchronized sampling, the sample acquisition rate is under the control of the user and could be as high as the waveform sampling frequency, which is generally not the case for synchrophasors.

Per the differences above, there is a definite advantage in using synchronized sampling rather than synchrophasors for fault location.

Once a fault occurs on a transmission line, there is no guarantee that the event reports at the two ends of the line will start at exactly the same instant in time. When using synchronized samples from two locations, it is necessary to align the samples. Figure 7 shows an example where there is a difference of four sampling intervals between the event reports collected at two substations. Figure 8 shows the aligned data where four samples have been removed from event report 1 in order to align the samples.

Once the samples have been aligned, the user can process the instantaneous samples at both locations through the same filtering system and the obtained phasors are automatically synchronized.

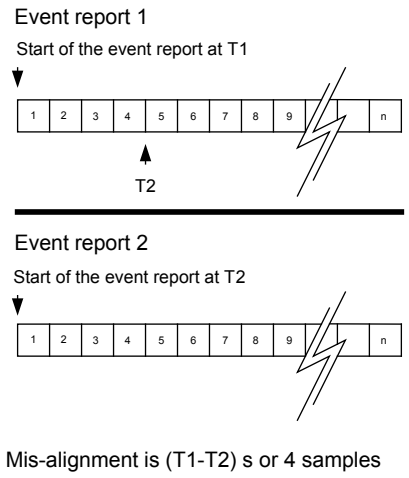

Figure 7—Principle of event report misalignment

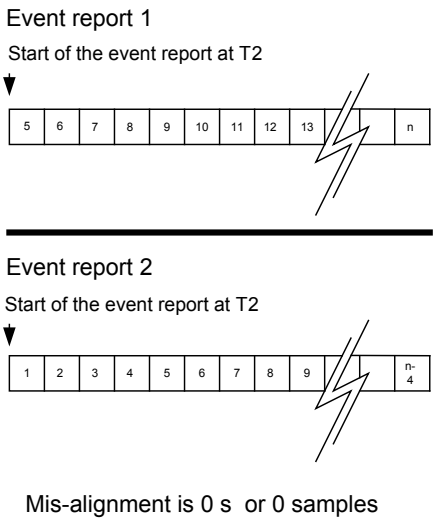

Figure 8—Principle of event report alignment

Figure 9 shows a real-world trajectory of the distance to the fault (in per unit of line length) for a fault that was caused by a brush fire under a transmission line. The primary fault resistance trajectory is shown in Figure 10 in primary ohms. As can be seen in Figure 10, the fault resistance was varying from a higher to lower steady-state value.

Both event reports were sampled at 960 samples/s and the phasors were acquired at the same rate. There was a time difference in the start of the event reports of four samples. Figure 9 shows the distance to the fault trajectory calculated with non-aligned and aligned samples. The plot shows the fault location with the aligned samples converges more rapidly to the final value. The distance to the fault is computed using Equation (27).

In conclusion, when synchronized sampling is being used for the purpose of fault location, one has an interest in using the highest sampling frequency possible to reduce the error when aligning the sampled data. This is because when aligning the data the synchronizing error is equal to the inverse of the sampling frequency.

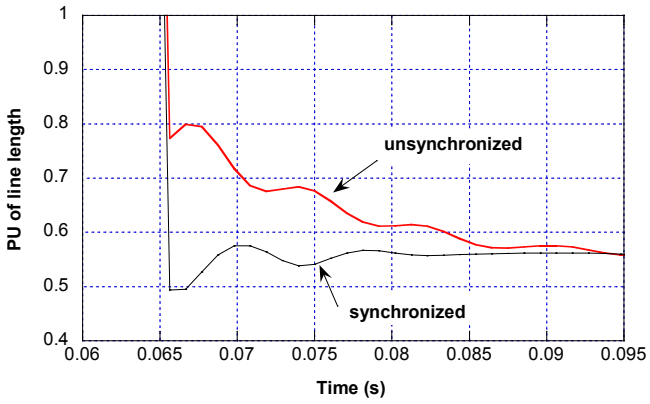

Figure 9—Distance to the fault trajectory from left side with synchronized and un-synchronized samples

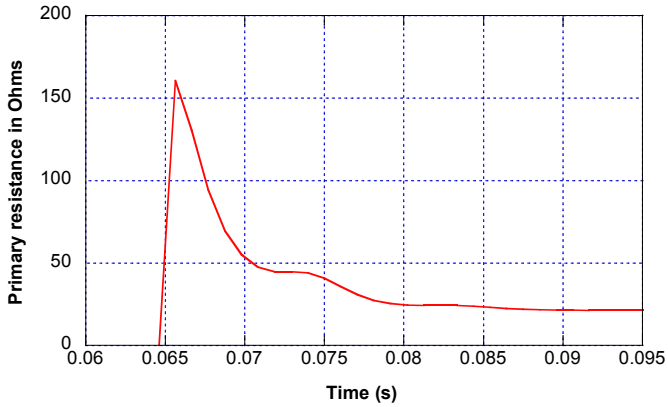

Figure 10 —Primary fault resistance trajectory

5. Other fault location applications

5.1 Three-terminal lines

Locating faults on three-terminal lines becomes more complicated, but methods have been developed to deal with the problems associated with them (Girgis, Hart, and Peterson [B10], Tziouvaras, Roberts, and Benmouyal [B61]). One of the first issues to arise when trying to locate faults on three-terminal lines is the setting of the line impedance in the fault locator. The impedance directly from one terminal to either of the other two terminals is chosen. Then, the apparent impedance of the leg to the remaining terminal is determined as a percentage of the original impedance selected. It is important to keep in mind that the apparent impedance will change for different system conditions.

Any faults on the line from the fault locator terminal to the tap point for the three-terminal line should be located correctly. If there is no infeed from the third terminal, the location of faults on the portion of the line beyond the midpoint would also be located correctly. However, any faults from the midpoint to the third terminal, or any faults involving infeed, would yield results in the fault locator that might be confusing.

A chart or nomograph can be compiled to accommodate the known infeed conditions. If a fault occurs on one of the portions of line beyond the midpoint and the infeed currents are as expected, the fault location can be looked up on the chart or nomograph. There will be two possible locations for the fault since it could be on either line section after the midpoint. One of the pitfalls for this method is that if the system configuration changes, the infeed currents would be different than anticipated. Thus, the results of the fault locator would no longer correspond to the chart or nomograph and would not be accurate.

If there is a fault locator at each end of a three-terminal line, the fault locator on the section containing the fault is the most accurate of the three.

The method described above requires additional work and analysis to achieve results. Techniques have been presented (Tziouvaras, Roberts, and Benmouyal [B61]) that use the negative-sequence network and can convert a three-terminal problem to a more conventional two-terminal one. Fault location can then be solved without any synchronizing requirement.

5.2 Series-compensated lines

Fault location on systems with series-compensated lines is considered to be one of the more difficult tasks for manufacturers and utility engineers (Novosel, et al. [B40]). Series capacitor banks cause steady-state and transient problems to impedance-based fault locating. Fixed series capacitors and thyristor controlled devices introduce harmonics and nonlinearities which adversely impact the protection function. Performance of protection systems and fault locators depend on the status of the capacitor and the transient response of the capacitor protection circuit. To take full advantage of the series capacitor installation in a network, it is necessary to explore the impact of series capacitors on fault location and implement appropriate fault location methodologies (Fecteau, [B6] Fecteau, Larose, and Deguire [B7], Saha, et al. [B50] Yu, et al. [B63]).

The addition of series compensation to a system will introduce several transient effects in estimating the voltage and current phasors. These effects impact fault location measurements for the series-compensated line as well as protection and fault locating on adjacent lines. These phenomena include the following:

— *Subsynchronous frequencies:* The capacitor will introduce a subsynchronous frequency. The frequency is dependent on the capacitor and system parameters. The natural frequency is proportional to the degree of compensation and is inversely proportional to the source impedance ratio and the fault location. Higher frequencies occur when the fault is close to the measurement device. The higher frequencies will not be as critical for close in faults since the capacitor metal oxide varistor (MOV) will typically short the capacitor for these cases. However, when a fault occurs near the end of the line the lower frequency components will cause the impedance estimate to oscillate.

— *Metal oxide varistor (MOV) and overload protection operation:* Once a fault has occurred, the bypass circuit breaker will be closed following operation of the overload protection system. This will introduce a transient in the system as the breaker contact arcs and the impedance seen by an impedance-based fault location algorithm is altered. The effect will be to increase the impedance to the fault and lower the fault current, thus altering the phasor estimate. A quick response of the MOV will reduce the capacitance and limit the impact of the sub-frequency component. Tripping of the overload protection circuit removes the capacitor from the fault loop.

— *Phasor estimate:* In addition to the above, asymmetrical gap flashing, high-frequency components, and other phenomena are expected to influence phasor estimates. Impact of high-frequency components is usually reduced by filters. Asymmetric gap-flashing mainly depends upon the operation and design of the MOV overload protection and has an effect similar to an unbalanced fault. Three-phase bypassing is very common, thus reducing the asymmetric gap-flashing effect. Proper filtering and measurement techniques are needed to improve phasor estimates and reduce errors caused by subsynchronous frequencies and other transient effects.

Performance of fault locators depends on the status of the capacitor and the transient response of the capacitor protection circuit. A simplified capacitor protection scheme is shown in Figure 11 (Goldsworthy [B11]). The MOV starts conducting immediately after the instantaneous voltage across the capacitor exceeds a certain voltage level V. The voltage versus current characteristic of a MOV is approximated by the single exponential model shown in Equation (30):

$$I = I_{\max}\left(\frac{V}{V_{pl}}\right)^{\alpha} \tag{30}$$

where

$I_{\max}$ is the maximum current for the MOV

V is peak voltage across the capacitor

V_{pl} is the protective (peak) voltage level of MOV

The value of alpha is typically chosen between 30 and 50. The MOV is a resistive device which absorbs energy and is protected from overheating by an overload protection scheme which calculates the energy developed through the MOV and initiates protective gap flashover (bypassing the MOV). In addition, a high-current function is provided to speed-up bypassing for severe internal faults if the current is much greater than I_{max}.

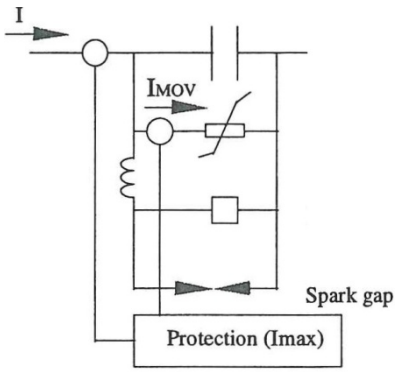

Figure 11—Typical layout of an MOV-protected series capacitor

For impedance-based fault locating, the location of the potential transformers on the line side of the series capacitor for use by the fault locator can eliminate the steady-state problem. In Figure 12 the potentials are on the line-side of the series capacitor. This is desirable and no steady-state problems will exist with this arrangement.

In Figure 13 the potentials are on bus side. This causes a steady-state error due the voltage rise between the measured bus voltage and the line voltage for a fault out on the line.

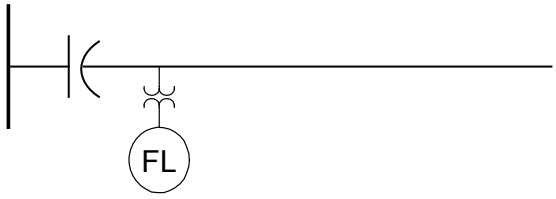

Figure 12 —Series-compensated line with line-side voltages

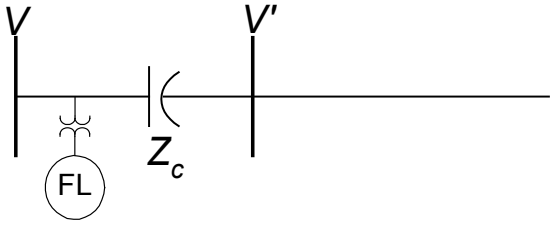

Figure 13 —Series-compensated line with bus-side voltages

Consider a fictitious bus on the line side of the capacitor (V'). The voltage at this bus can be calculated using the measured phase currents, voltages, and capacitor impedance as seen in Equation (31):

$$V' = V - Z_C I \tag{31}$$

Without an MOV, Z_C is capacitive impedance at –90°, which will cause a voltage rise at the fictitious bus compared to the substation bus voltage for current flow out onto the line. With MOV, V_C depends on MOV response and is zero when the spark gap protection on the capacitor fires and bypasses the bank.

The transient problem is caused by the fact that energy is stored in both the inductance of the system and the capacitance of the series capacitor. A fault on the system disrupts the equilibrium of this stored energy, which produces oscillations. The frequency of the oscillation is determined by the natural frequency associated with the value of the inductive and capacitive reactance of the system. This oscillation damps out, but not during the normal fault clearing time for a high voltage transmission line. During the transition, the line current waveforms include two components: the fundamental sinusoidal component of the driving voltage and the damped sinusoidal component at the natural frequency of the system. This combination produces a modulated waveform that is oscillating at the difference between the fundamental frequency and the natural frequency of the system. Figure 14 is a waveform captured on a digital fault recorder. The waveform is a phase current at a line during a fault on a 500-kV series-compensated system.

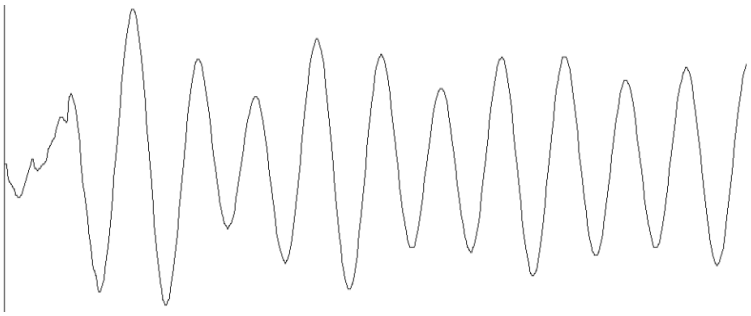

Figure 14 —Phase current on a series-compensated system

It is clear that the magnitude is not remaining constant and that, although the low-frequency component of this waveform shows signs of damping, a steady-state value for this current has not been reached at the end of the record. Since fault study programs calculate the steady-state value of the current and voltage during a fault condition, the fault study calculated current for this fault condition is significantly different than the magnitudes of the first few half cycles of this fault current. Normal fault clearing occurs in the first four cycles on high voltage transmission lines. This slow damping of the low-frequency transient makes fault study current comparison impractical for fault locating on this line.

The faulted phase voltage at the substation for this fault had a relativity constant magnitude, so the apparent impedance from the substation to this fault was varying with the low-frequency oscillation of the current. These transients are difficult to filter because signals are at frequencies lower than the fundamental frequency of the system. The oscillation of the apparent impedance makes impedance-based fault locating for this series-compensated line impractical.

If the series capacitor's protection operates (gaps flash) for a fault, the oscillations are damped quickly and impedance or current-based fault locating will provide fault locating as accurate as for other uncompensated lines. The system from which the waveform in Figure 14 was recorded has two 67 Ω series capacitors in the line and there are large sections of the line for which faults will not cause (one or neither) of the capacitor banks' gaps to flash.

The low-frequency oscillations of the current produces peak values that are higher than the predicted steady-state fault current. The higher currents cause the protection on the series capacitor bank to operate for faults in locations the steady-state studies would not have predicted. If the series capacitor bank is protected with gaps, the capacitor bank would be completely shunted when the protection operates, but if it is protected with metal oxide varistors (MOVs) the capacitor bank is only shunted during the current peak values. The operation of the MOVs creates impedance for the capacitor bank that looks like a variable resistor in parallel with a capacitor. The value of the variable resistor is changing during the waveform of the current through the series capacitor bank. If the location of the fault is trying to be determined by monitoring the current that is passing through the capacitor bank, the results are disappointing.

Fault locating using current or impedance measuring methods has proven to give some degree of accuracy if the impedance of the bank is relatively small and the protection limit of the capacitor is low compared to the available fault current. The following is an example of such a case.

In this example the magnitude of the current is used in a graphical method to determine the location of line faults. The transmission line is a 260.7-km long, 500-kV line with 26% series compensation. All of the series compensation is located at the Station 1 end of the line. Shunt reactors are located at both ends.

As illustrated in Figure 15, the line distance given in percent is from the left side, or Station 1 bus, to the right side, or Station 2 bus, and is plotted horizontally on the graph. Current magnitudes in amperes are plotted vertically. The curves were developed from fault studies. Gap flashing ceases for current levels below 5650 A.

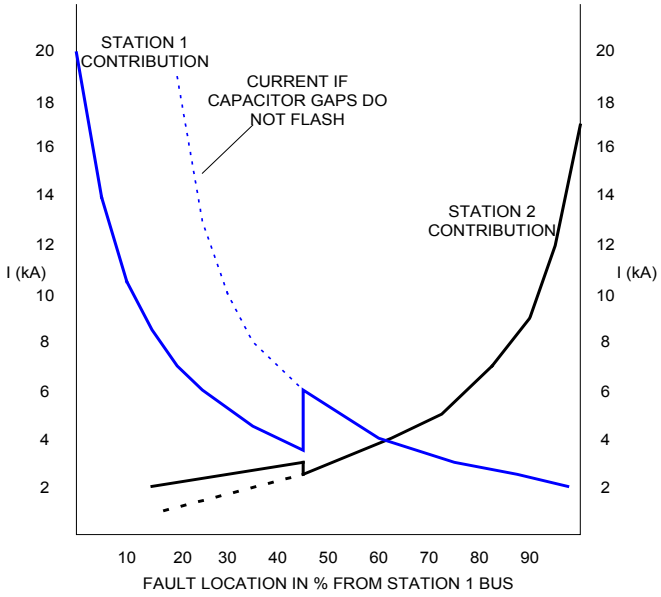

Figure 15 —Series compensation located at one end only

Using only a single-end current contribution curve may not provide sufficient information to locate a particular fault. For example, using only fault recorder information from Station 1, it can be seen that for a 5000-A fault, two possible fault locations exist. One location could be at 32% of the line if the gaps flash and another at 53% if the gaps do not flash.

Since the location of the fault may plot at different distances, depending on which current contribution curve is used, a midpoint between the two values is chosen as the probable location. For example, using Figure 15, if the location plots at 40% of the Station 2 current contribution curve (2800 A) and the location plots at 30% on the Station 1 current contribution curve (5200 A), then the fault location is selected as at 35% of the transmission line. Ideally, the Station 2 current contribution should be 2400 A. However, error due to differences in calculated impedance from actual line impedance affects the true value.

If the voltage measurement is on the line side, the accurate approach could be to estimate the voltage across the series capacitor by taking into account the MOV response (Goldsworthy [B11]). Modeling of the nonlinearity of the MOV-protected series capacitor installation using only the measured line current and bus voltage is described in (Peterson, et al. [B44]). The voltage across the capacitor is calculated and then used to determine the line side voltage of the capacitor by summing the measured bus voltage and the voltage across the capacitor, as shown in Equation (31). The calculated line side voltage can be used with

any of the other fault location techniques. Accurate fault location requires detecting if the capacitor is not in service or if it is bypassed by the spark gap.

Furthermore, in general, traveling-wave techniques as described in Clause 6, provide accurate fault location. This technique is incorporated in fault locating devices and some manufacturers are incorporating traveling-wave fault location algorithms into their protective relays. Although there are various other techniques such as: phasor based (impedance, voltage, or current based), time-domain based (synchrophasors), wavelet based, and others that have been developed these techniques are seldom used for locating faults on series-compensated lines.

Annex B provides additional theoretical information on locating faults on series-compensated lines.

5.3 Parallel lines

Fault location estimation for the parallel lines may be influenced considerably by the mutual coupling effect for a ground fault. If the fault current and the parallel line current are in the same direction, fault location will overestimate and vice versa. In general, lines that have zero-sequence mutual coupling with parallel lines are not well suited for one-ended fault locating. If lines are parallel for the entire line length, as shown in Figure 16, the following conditions are usually considered for the fault location estimation:

a) One of the parallel lines is switched off and grounded at both ends (Breaker 3 and Breaker 4 are open). Since the fault current and the residual current from the parallel unfaulted line (I_{RM}) flow in opposite directions, the fault locator will underestimate.

b) Both parallel lines are in service. Since the fault current and the residual current from the parallel unfaulted line (I_{RM}) flow in the same direction, the fault locator will overestimate.

c) The fault locator on the healthy parallel line is compensated with the current from the faulted parallel line. This will cause the fault locator to underestimate.

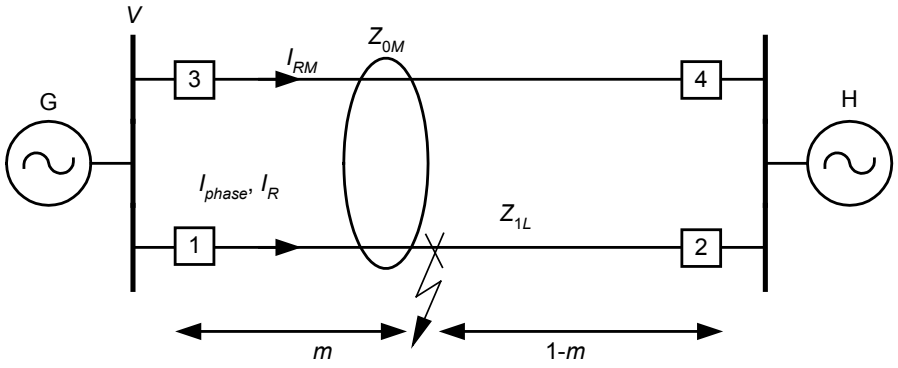

Figure 16 —Impact of mutual coupling on fault location for parallel lines

The voltage drop compensation by the residual (zero-sequence) current in the parallel circuit, I_{RM}, for an A-phase-to-ground fault is expressed as shown in Equation (32):

$$V_A = mZ_{1L}\left(I_A + k_0 I_R\right) + mZ_{0M} I_{RM} + R_F I_F \tag{32}$$

However, most lines are not parallel for the entire line length. Figure 17 represents some typical system arrangements.

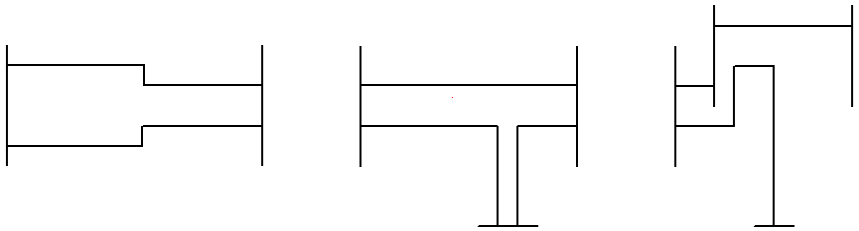

Figure 17 —Parallel line configurations

Suggestions for approaching zero-sequence mutual fault location errors include the following:

a) Calculate the effects and make a correction chart or charts. For example, a short-circuit program may be used to generate voltage and current data for faults along the line of interest as input to the apparent impedance equations (Table 1) given earlier. Then construct a graph comparing theoretical fault locations with actual fault locations (e.g., nomograph).

b) Use two-terminal methods to compensate for the mutual effect. Techniques have been presented (Tziouvaras, Roberts, and Benmouyal [B61]) that use the negative-sequence voltage and current phasors from both extremities, without synchronizing requirements.

c) If only local data is available and lines are parallel for the entire length, use the residual current from the parallel unfaulted line and zero-sequence mutual impedance (Z_{0M}) to compensate for the voltage drop to the fault caused by mutual coupling.

5.4 Tapped lines

In the case of tapped lines, the measurement used for the fault location algorithm may not be available at each end of the tap. This case may be designated as a “sparse measurements” case. In such instances, the fault location may be determined by matching the short-circuit solution with the measurement at the point where the measurement exists. The fault location is varied until the voltages and currents between the simulated and measured phasors are nearly the same. The fault location determined from the short-circuit program is the one that is the actual fault location in the field. An optimization technique was developed to resolve this ambiguity that was field tested and shown to provide good results (Kezunovic [B25]).

5.5 Distribution system faults

5.5.1 Background

Practical fault location methods based on the use of current and voltage phasors have been implemented in the feeder protection devices. The reliability and accuracy of substation-based fault locators is questionable because of numerous factors. Some techniques that can reduce errors will be discussed in the following paragraphs.

The unique topography of solidly grounded distribution systems presents many challenges for fault locators at the substation. These include:

a) Conductor sizes change, thus making impedance calculations nonlinear. One possible solution is to model the line and create a nomograph.

b) Multiple feeder taps and laterals.

c) Inaccurate models/system data and dynamic configurations can affect results.

d) Less energy to establish clean arcs.

e) Evolving fault characteristics and magnitudes can fool a relay's ability to select the correct fault type.

In the case of a phase-to-ground fault, the reactance algorithm using the zero-sequence voltage and the zero-sequence current of the faulted feeder may be used to compensate for the effect of the tapped loads with wye-delta distribution transformers. Subclause 5.8 discusses the effect of tapped loads in more detail. Another approach is to use the capacitive current of the feeder (important if a large portion of the feeder consists of cable). One can also improve the fault location for ground faults by using the ground or residual current (I_R) instead of the faulted phase current (I_G) in Equation (13).

Another method uses an online calculation of the source impedance (behind the IED) and the load impedance to compensate for the tapped loads (in addition to a complete compensation for the reactance effect) in a radial distribution network. The load impedance is calculated using the pre-fault data shown in Equation (33):

$$Z_{\text{load}} = \frac{V_\ell}{I_\ell} - Z_\ell \tag{33}$$

where

V_ℓ and I_ℓ are pre-fault load voltage and current

Source impedance behind the fault locator is calculated from the fault and pre-fault voltages and currents at the terminal as shown in Equation (34):

$$Z_S = -\frac{\Delta V_G}{\Delta I_G} \tag{34}$$

Since the system is radial, by calculating Z_ℓ and Z_S, the value of β is accurately calculated as shown in Equation (7). Once the value of β is accurately known, this method (using only local measurements) can compensate completely for the errors caused by the reactance effect without requiring input of a source impedance as a setting parameter. Compensation for tapped loads allows this method to provide accurate results for a variety of fault cases on distribution feeders, although the accuracy may degrade for faults occurring toward the end of the feeder.

Distribution networks can have different grounding principles, which affect the means to determine fault location. Grounding principles can be as follows:

a) Solidly grounded

b) Ungrounded networks

c) Peterson's coil

d) Resistance grounded

5.5.2 Solidly grounded networks

5.5.2.1 General

Of the four types of grounding listed in 5.5.1, the solidly grounded network is the most common in North America. The ungrounded network will require grounding transformers, which are distributed around the network resulting in fewer sources of ground current. The net effect of this, and of the latter two types of grounding, is to reduce the magnitude of the ground current. This can be seen as an increase in zero-sequence source impedance. Techniques to locate faults on these networks will not differ from those shown for solidly grounded networks except for the reduced accuracy of the computational techniques.

5.5.2.2 Fault-location technologies

5.5.2.2.1 Traditional methodologies

Often faults are located without the use of any measurements. Location is simply made through physical indications, field methods, and use of information such as the following:

a) Restoration through switching
b) Restoration through recloser operation
c) Indication through fuse and fault locator operation
d) Downed wires, customer/fire/police calls, maps
e) Relay targets
f) DC thumping of underground circuits
g) Smelling burnt cables

5.5.2.2.2 Observant technologies

The ability to collect data further improves upon the success of locating faults through such techniques as the following:

a) Local detection with communications feedback
b) Intelligent metering with modem, cellular-based devices, LOCATE-type devices
c) Detectors sending feedback through supervisory control and data acquisition (SCADA)
d) Satellite-based location or carrier packages
e) Choice of passing on information to an “interpreter” (i.e., a person) or to an “interpretive device” (i.e., a substation human-machine interface or distribution management system)
f) Use of distribution management/operations systems with customer call information
g) Fault recorders

5.5.2.2.3 Intelligent technologies

Due to complexity, intelligent technologies are being applied for distribution fault location. These include the following:

a) Artificial intelligence, neural networks to "learn" system characteristics

b) Distributed intelligence in substations to pull together information for best guess, confidence factors

Although evolving, competition may arise among observant technologies dispersed throughout the system, but integrated together, and advanced intelligent technologies.

5.5.2.3 Application of distribution fault locating

Although fault location on distribution feeders can be more challenging than transmission systems, there have been many applications where fault locating on distributions systems has been very successful. For example, one utility in the Midwest United States has implemented a system that has resulted in a 90% success rate in accurately locating distribution feeder faults. The system measures the current on the feeder bus main breaker or transformer low-side breaker that is supplying all of the distribution feeders (see Figure 18). Instead of using the fault-locating algorithm in the relay they determine the fault location from the measured current in the relay which is an output of the fault record. Short-circuit studies are performed at a number of locations on the feeder(s) and the information is stored in a database. When a feeder operates, the measured current seen by the feeder bus main breaker or transformer low-side breaker is used to determine the fault location from the previously stored database of fault locations for that feeder. This utility has found that the currents from the feeder main breaker and the currents on the faulted feeder compare very well and that the majority of their distribution faults have no or very low fault resistance, so they have excellent results in successfully locating faults.

In many instances of such applications the fault location algorithm may not be able to differentiate between faults at two different locations since the conditions for matching the measurements to the simulation results appear to be the same. An optimization technique that helps resolve this ambiguity is developed and tested and shows definite advantage (Dong, Zheng, and Kezunovic [B4], Kezunovic [B25], Lotfifard, Kezunovic, and Mousavi [B32], Lotfifard, et al. [B33], Pereira, Kezunovic, and Mantovani [B42], Pereira, et al. [B43]).

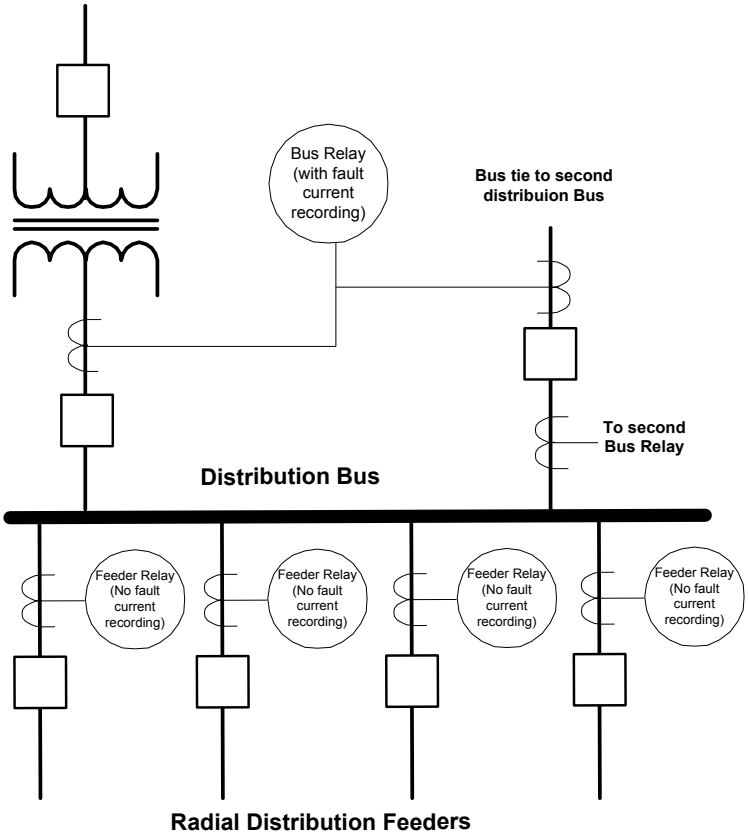

Figure 18 —Distribution system example

5.5.2.4 Fault location for distribution feeders

A typical distribution feeder has multiple laterals tapped off the main three-phase feeder at different locations. Figure 19 illustrates the structure of a typical distribution feeder. The solid lines indicate the three-phase sections and the dashed lines indicate the non–three-phase sections. The line sections that compose the distribution feeder may have different X/R ratios because of the different types of conductors. Considering the nonhomogeneous line impedance characteristics and the tree-type topology of distribution feeder, several fault impedance-based and fault current-based profile methods have been developed (Zimmerman and Costello [B64]). However, these methods are mainly manual processes and the numbers of branches that can be included are often limited. Fuses, reclosers, and sectionalizers can also assist in the fault location processes as these devices may operate for the fault to provide additional information on the fault location.

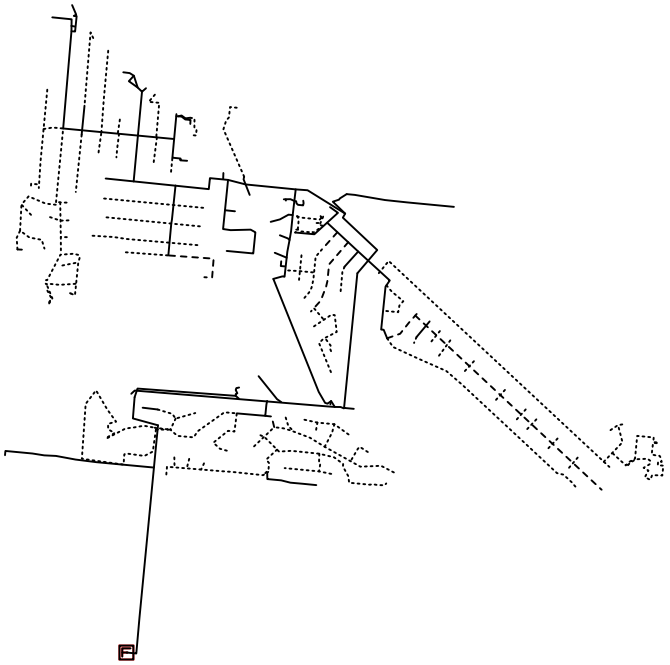

Figure 19 —Typical distribution feeder with multiple branches

An improved fault location method is presented in Gong and Guzmán [B12] to facilitate the fault location process for distribution feeders. This method uses Equation (35), Equation (36), and Equation (37) to calculate the total reactance between the fault and the location of the measurement device, depending on the type of fault. Equation (35) is for single-phase-to-ground faults. Equation (36) is for phase-to-phase and phase-to-phase-to-ground faults. Equation (37) is for three-phase faults. This method eliminates the impact of fault resistance and reduces errors due to mutual coupling and loads.

$$X_{total} = \frac{\mathrm{Im}(V_{faultedphase} \times I_2^*}{|I_2|^2} \tag{35}$$

$$X_{total} = \mathrm{Im}\left(\frac{V_2 - V_1}{2 \times I_2}\right) \tag{36}$$

$$X_{total} = \mathrm{Im}\left(\frac{V_1}{I_1}\right) \tag{37}$$

The fault location system presented in (Gong and Guzmán [B12]) imports the detailed feeder model from commercially available distribution system analysis software package and uses a search algorithm to automatically find potential faulted line sections that meet the reactance criteria. This system can also incorporate the operational information from field devices, such as faulted circuit indicators (FCIs) and recloser controls, to further improve the fault location accuracy by reducing the number of possible fault locations. The fault location result is displayed on a map to assist in locating the fault, as illustrated in Figure 20.

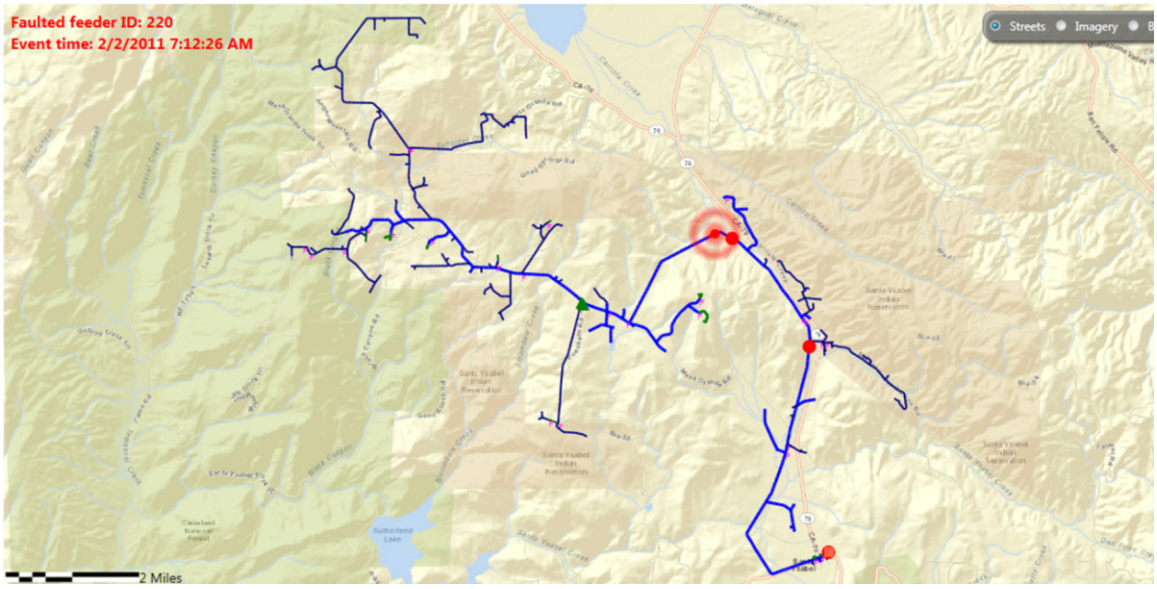

Figure 20 —Display fault location result on map to expedite locating fault

5.5.3 Example application of networked underground distribution fault location system

5.5.3.1 Background

This case study presents a distribution fault location system in production use at an investor-owned electric utility with a distribution system that is more than 85% underground. The fault location system incorporates substation bus power quality monitors, feeder digital relays, distribution circuit models, relational databases, GIS data, and SCADA operation records. The estimated fault location is within three manholes for about 80% of the SLG faults recorded by the system. More detailed information about this automatic fault location system is provided in (Sabin, et al. [B47]).

5.5.3.2 Data collection

For the electric utility that is the focus of this case study, distribution substations supply the distribution network feeders with line-to-line voltages of 13 kV, 27 kV, or 33 kV. The bus in each substation is typically supplied by four transformers. Most substations have a fifth transformer that is normally open-circuited on hot standby. Together, the four transformers typically deliver 50 to 200 MW to distribution feeders that supply a distributed secondary network. There is a power quality monitor at the output of one transformer in each substation. The substations are grounded using neutral reactors to limit fault current, so a significant amount of zero-sequence current is seen during single-phase-to-ground faults. Many substations have more than one transformer with a power quality monitor to allow for redundancy in data collection. See Figure 21.

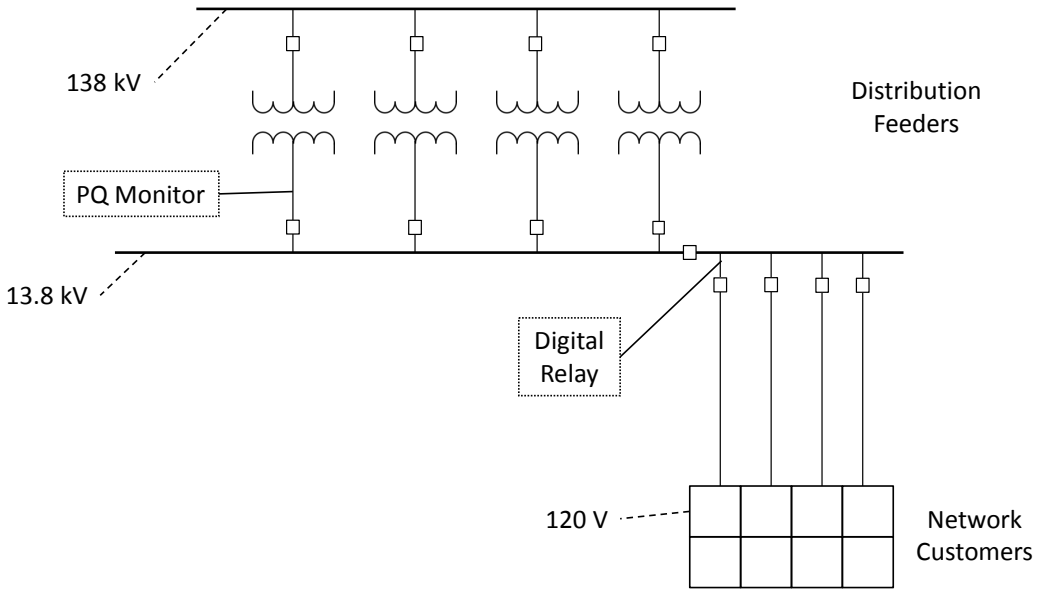

Figure 21 —Location of power quality monitors and digital delays in underground distribution monitoring system

The power quality monitors in the substations are configured to record waveform samples during the voltage sags caused by system faults, such as the measurement displayed in Figure 22. The power quality monitors provide voltage and current waveform samples during faults at a rate of 128, 256, or 512 points per 60-Hz cycle, and have their sampling rate synchronized to the line frequency. At most locations, the monitors record phase-to-neutral voltages (i.e., VAN, VBN, and VCN) and the line current (i.e., IA, IB, and IC).

The data for most of the power quality monitors is downloaded by telephone modem every ten minutes. Some substations have been configured with Ethernet access, which enables their polling frequency to be once every minute or faster.

Once downloaded from the substation, data from the power quality monitors is integrated automatically into a relational database. Some of the source data from the power quality monitors is in a proprietary binary file format that requires special handling. However, many of the newer power quality monitors produce data in the IEEE PQDIF binary file format (IEEE Std 1159.3™-2003 [B16]) making measurements very accessible.

The network feeders supply transformers that in turn supply a low voltage distributed secondary network. The network feeders are protected using overcurrent relays. A minority of the feeders is monitored using a digital relay that can be polled for measurements during feeder energizing, breaker trip events due to fault events, and short-duration overcurrent faults due to incipient fault events.

Data is downloaded from digital relays using customized scripts via a frame relay wide area network. The data files from the relays are converted to either the binary or ASCII format specified by the IEEE COMTRADE file format (IEEE Std C37.111™-1999 [B17]). The digital relays provide voltage and current waveform samples at 32 points per cycle.

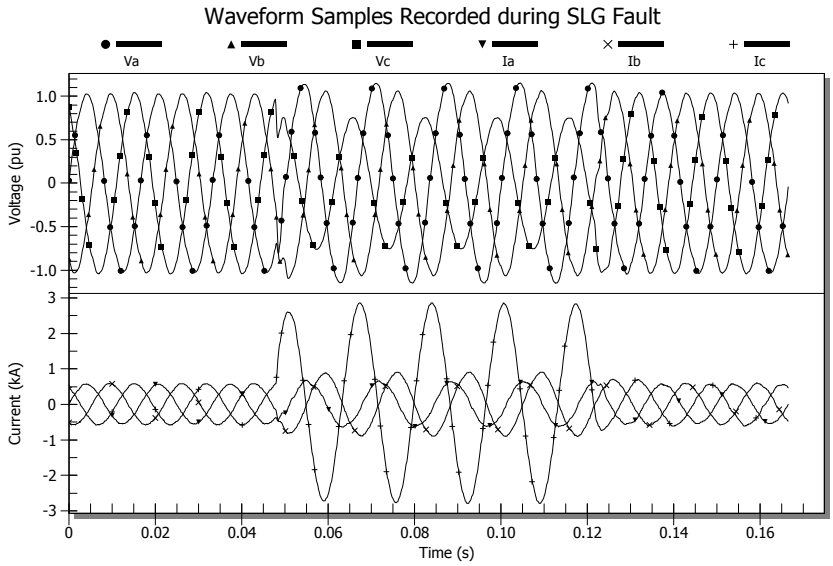

Figure 22 —Voltage and current waveform samples recorded for a ground fault

5.5.3.3 Data integration and fault analysis

Each measurement is analyzed automatically with commercial software, which can classify each measurement as more than one type of fault. This means that the system is able to identify single-phase faults that evolve into multi-phase faults. As another example, the system is able to identify the start and end of each stage of a fault that begins as transformer energizing transient but degrades into a fault condition.

Every measurement recorded by a power quality monitor or digital relay is correlated with circuit breaker open and close operations recorded by the SCADA system, which are stored in a historian server. When a positive correlation between a waveform record and a SCADA record is found, information describing the circuit breaker operation is stored in the relational database with the waveforms.

5.5.3.4 Reactance-to-fault estimation

For single-phase faults, the reactance-to-fault (XTF) is estimated using Equation (38), where V_f is the magnitude of the voltage measured on the phase showing a voltage sag, N_T is the number of transformers in service during the fault, I_0 is the magnitude of the zero-sequence current, and is the phase angle between V_f and I_0. The reactance is divided by the number of transformers in-service at the time of the fault because each power quality monitor is monitoring the output of a transformer supplying a bus rather than directly monitoring the current for the faulted feeder. When working with relay data from the feeder itself, the division of the reactance is not needed.

$$\mathrm{XTF} = \frac{V_f}{N_T k_1 I_0} \sin\theta \tag{38}$$

The constant k_1 is a calibration factor that is determine uniquely for each substation and for each feeder. It is derived using previous faults recorded at the substation in the recent past using historical faults on a feeder when the network was in the same configuration for the fault that occurs in the present. Practical use of the fault location system indicates that the actual distance in reactive ohms for historical faults can be

used to determine a value of k_1 that will estimate the reactance-to-fault for future events. The k_1 constant can be computed at the bus level for all feeders supplied by a substation, or can be computed for each feeder. The feeder-level k_1 constants typically are more accurate than the bus-level constants. Figure 23 presents the magnitude of the voltage and current phasors derived from Figure 22, along with the reactance-to-fault computed using a k_1 constant of 5.5.

The distribution circuit models are provided by a load flow application developed and maintained by the electric utility. Each feeder is modeled within the load flow application using conductor type and connectivity data in order to create tables of impedance between substation and structures (for example, manholes and vaults). The model provides positive-sequence impedance only, which necessitated the usage of positive-sequence reactance for single-line to ground (SLG) faults rather than a loop reactance using a combination of the positive-sequence and zero-sequence.

For multi-phase faults, a more traditional method is used for fault location. The approach described in this document for single-ended impedance-based measurements has been applied successfully to the distribution faults measured in this underground network. This method requires computation of phase-phase voltage and phase-phase current phasors before the fault and during the fault.

Table 2 presents a summary of the estimated fault location versus actual fault location for SLG distribution faults as recorded at substations.

Table 2—Percentage of SLG faults catagorized by distance in manholes between estimated fault location and actual fault location

	Distance in manholes				
Year	**< 1**	**1 to 3**	**3 to 5**	**5 to 10**	**> 10**
2007	67%	16%	7%	6%	4%
2008	67%	16%	6%	4%	8%
2009	64%	23%	5%	2%	6%
2010	67%	20%	8%	3%	5%
2011	64%	14%	4%	4%	1%

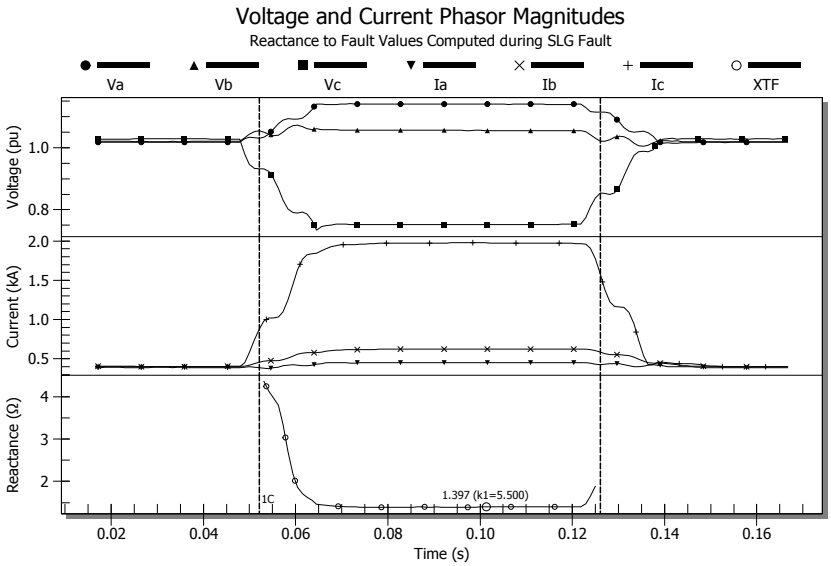

Figure 23 —Voltage and current phasors computed from the fault shown in Figure 22

5.5.3.5 Fault location visualization

On the electric utility's corporate intranet, several applications provide operations and engineering with estimated fault location. For example, one report displays a summary page with the number of faults detected at different substations. The count of faults, inrush events, and subcycle faults is shown separately. Hyperlinks are provided in the web page to other reports that provide more detail. One report shows the estimated reactance-to-fault for each fault measurement that is matched with the reactance data from the feeder that operated. A table in the report provides hyperlinks to an online web map, Figure 24, displaying the one-line diagram for the cable that operated.

Colors are used to highlight the estimated location, with one color being used to highlight the node that is closest to the estimated location and other colors being used to indicate other possible fault locations. Initially, the visual fault locator web application only showed one possible location, but it was found useful later to have additional colors in order to encourage field personnel to look upline or downline of the estimated location.

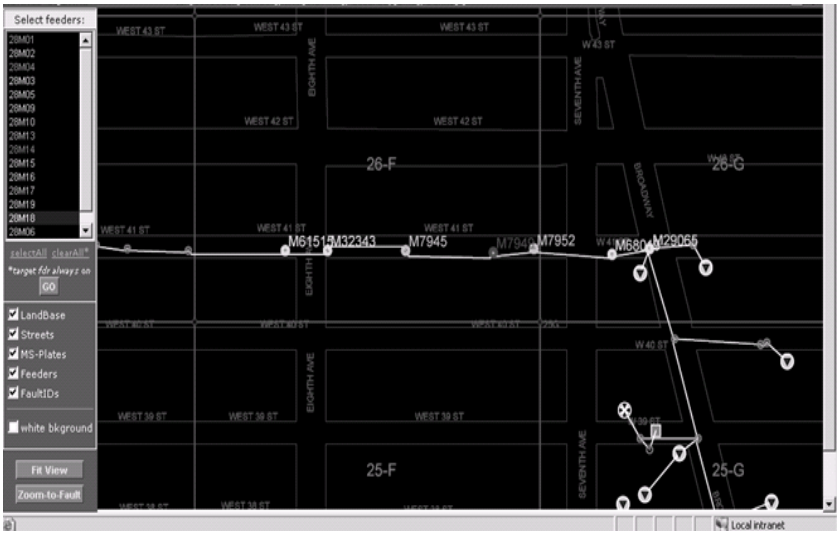

Figure 24 —Example of intranet web application displaying estimated fault location

5.6 Locating faults on underground cables and paralleled cable circuits

5.6.1 Underground cables

Locating faults on underground transmission or distribution cables is difficult to achieve using microprocessor relays. First, the zero-sequence impedance changes due to distributed shunt capacitance along the entire cable (see Figure 25). The capacitance can change depending on the system voltage, stored charge, different zero-sequence return paths, and other factors. The effect can be likened to infeed from unpredictable sources along an entire transmission line. Moreover, the ohmic value of the cable is usually small, so a minute error in the impedance model results in large errors in predicting fault location.

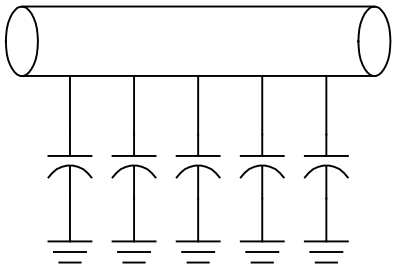

Figure 25 —Distributed capacitance along underground cable

In practice, utilities use some form of pre-location followed by one or more methods to pinpoint the location of the cable fault. The methods used depend primarily on voltage class (transmission or distribution) and installation (conduit or direct burial).

There are generally two categories of fault locating: terminal methods and tracer methods. These methods of fault locating usually take place after a fault has occurred and has been cleared by protective relaying.

Terminal methods measure electrical quantities at one or both ends of the cable circuit. Terminal methods are usually used to "pre-locate" the fault. The most popular terminal methods include "bridge" techniques, like the Murray loop, and radar/low or high voltage pulse methods (Bascom, Von Dollen, and Ng [B2]).

Tracer methods are most useful for "pinpointing" the location of the fault, and usually require walking the cable route in the field. The most popular tracer methods are acoustic ("thumper") techniques and earth gradient (applying a source and measuring return current) methods, although many other methods are used (Bascom, Von Dollen, and Ng [B2]).

The transient voltage and current waves collected during the fault can be used to pinpoint cable fault locations on distribution circuits. The method measures the time between transient peaks to compute a distance to fault (Wiggins [B62]).

5.6.2 Paralleled cable circuits

Frequently, two conductors in parallel are used instead of one larger conductor. In the case of insulated cables, a cable failure is characterized as a line-to-ground fault on only one of the conductors. The line impedance in this case is not a linear function of the distance to the fault (see Figure 26). In the case of a radial circuit supplied from one side only, the impedance is related to the distance to the fault as:

$$Z = f(m) = m(2 - m) \tag{39}$$

where

Z is the normalized impedance to the fault (= 1 at the end of the line)

m is the per unit distance to the fault (= 1 at the end of the line)

In the usual case of sources at both ends of the line, the situation resembles a three-terminal line.

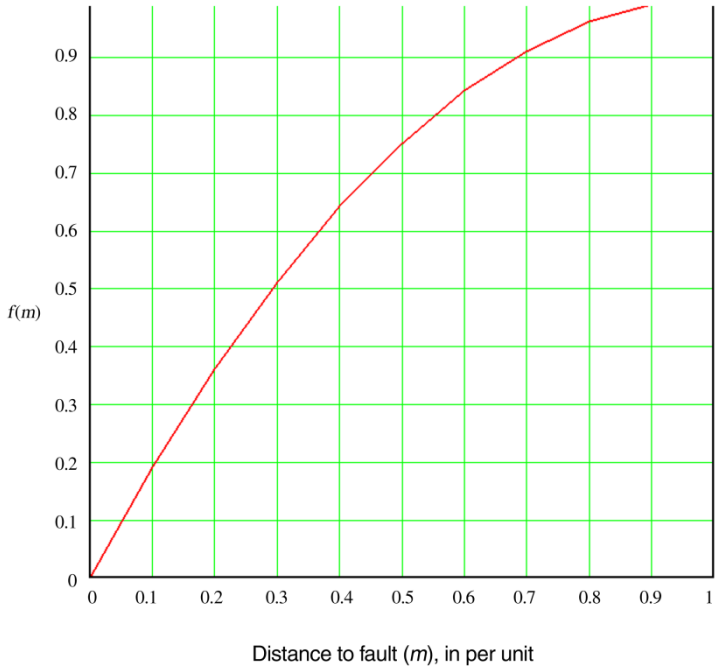

Figure 26 —Paralleled cable impedance changes with fault location

5.7 Automatic reclosing effects on fault locating

Automatic reclosing can affect the accuracy of fault locating, depending on the line configuration. The first fault usually provides accurate data because it usually has valid pre-fault and fault data. If reclosing into a de-energized line, the absence of load can actually help produce a more accurate fault location estimate, as long as the fault locator selects the correct data. Both two-terminal and one-terminal algorithms can be applied to locate faults. Automatic or supervisory reclose attempts into a permanent fault can (and most often do) have increased dc offset that can take several cycles to decay. This dc offset must be accounted for (e.g., filtering relay inputs) in order to accurately locate the fault.

5.8 Effect of tapped load

It is of interest to point out that while the effect of fault resistance could be reduced or even eliminated, its presence can magnify the errors contributed by other factors. A case in point is the configuration shown in Figure 27, which shows a one-line diagram of a three-phase fault at the end of a transmission line with impedance jX. A tap load of impedance $R_{LO} + jX_{LO}$ is connected close to the bus.

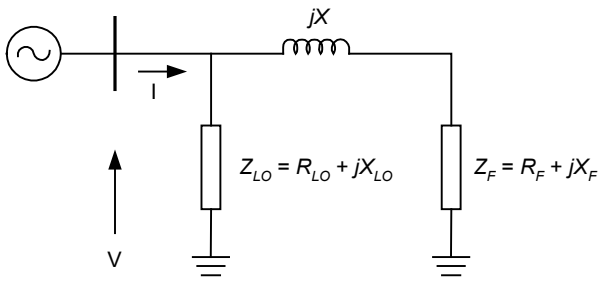

Figure 27 —Three-phase load affect on fault location estimate

The fault is through a fault impedance of $Z_F = R_F + jX_F$. The source impedance behind the bus is considered negligible. Analysis of this circuit with the Takagi algorithm results in an expression for fault location as shown in Equation (40).

$$\delta = \left[\frac{(X_F + X)}{X_m}\right]\left[\frac{1}{1 + \frac{R_F R_{LO}}{R_{LO}^2 + X_{LO}^2} + \frac{X_{LO} X_F}{R_{LO}^2 + X_{LO}^2} + \frac{X_{LO} X}{R_{LO}^2 + X_{LO}^2}}\right] \tag{40}$$

where

$\delta = \frac{X}{X_m}$ is the actual location.

It is observed that in addition to the inductive component of fault impedance contributing to direct positive error, both the resistive and inductive components of the fault impedance interact with the tap load impedance to augment the total negative error in the fault location determination. The above result was based on analysis of a three-phase fault. Testing with phase-to-ground and phase-to-phase-to-ground faults indicate that the error varies without consistency depending on the fault location (Marttila [B36]).

The above illustrates that while the effects of certain sources of error can be reduced with certain processes, the effectiveness of a process may be diminished by interaction with other factors.

5.9 Phase selection, fault identification, sequential faults

Fault location algorithms in protective relays typically use pre-fault and fault currents measured locally and stored in the memory of the relay. Under normal system conditions, the relay is measuring the currents and voltages for all phases and storing them in a buffer. Once the relay detects a fault condition in the zone of protection or initiates a trip of the line breaker(s), the data in the buffer are not updated anymore and are used to perform the fault location calculations.

The next step in a typical algorithm is the selection of current and voltage data to be used for the fault location calculation. A different loop is selected as a function of a faulted phase selection procedure. Many algorithms make the faulted phase selection based on superimposed components, this way eliminating the effect of the load on the phase selection.

The faulted phase selection decision is very important because if the wrong loop is selected, the results from the fault location algorithm will not be accurate. It will also affect the calculation because it is used in the determination of the fault inception point. A certain number of samples before and after the fault inception will be used to calculate the voltage and current phasors. If the faulted phase and fault inception point are not correctly selected, the calculated phasors will also introduce error in the estimation of the fault location.

Evolving faults introduce an additional problem, since they will usually require a switch from a single-phase-to-ground loop to a phase-to-phase loop. Two-phase-to-ground faults are typically evaluated as phase-to-phase faults in a fault location algorithm.

A three-phase or three-phase-to-ground fault can be considered as a combination of three phase-to-phase faults. The fault location is then determined for each phase-to-phase fault, and the closest to the relay location or the average of the three can be used as the output from the fault location algorithm. Some fault location algorithms may instead use a pre-selected phase-to-phase loop (for example a-b) in case of a three-phase fault.

Some relays use the same algorithm for fault location that is used by the distance protection function, but with a higher number of samples, which results in a better accuracy. Appropriate faulted phase selection is important in this case as well, because the resistance and reactance calculation is based on a single-phase or two-phase loop.

5.10 Long lines and reactor and capacitor installations

Long transmission lines on higher voltage levels may exhibit considerable capacitance resulting in a significant charging current. Shunt reactors or capacitors may be installed in the substations. If the fault location algorithms (one- and two-terminal) do not compensate for the shunt elements and the charging currents, an error may be introduced. Improvements in estimation can be accomplished by:

a) Compensation for charging currents and shunt reactors or capacitors by using a Π, Γ, or T line model

b) Compensation for long lines using a distributed line model

5.11 Short duration faults

Impedance-based fault locating methods require that the fundamental voltage and current quantities be accurately measured. This requires signal filtering and signals of long enough duration to measure. If faults clear faster than two cycles, the current may never reach its faulted steady state, and the voltage may never drop to its faulted steady state, so the fault locator tends to estimate long. Traveling-wave approaches may provide the only solutions.

5.12 Effect of untransposed lines on accuracy of line parameters

Transposition is the practice of rotating the positions of the phases of a transmission line at intervals so that each phase in turn occupies all positions in a given line configuration. This practice is prescribed in order to equalize the mutual inductances between the phases. A line divided into three segments such that each phase occupies each position for approximately 1/3 of the line length is considered fully or completely transposed. Calculations of line impedance parameters generally assume a fully transposed line in order to simplify the calculations. However, in order to keep the cost of construction down, many lines are actually built without transpositions. This naturally results in an unbalanced line with individual phase impedances

that are different from the calculated values, which are based on fully transposed lines. The error becomes significant for long lines resulting in increased error for fault locations based on single-ended impedance algorithms.

The following example will help to illustrate the situation. Consider the horizontal line shown in Figure 28.

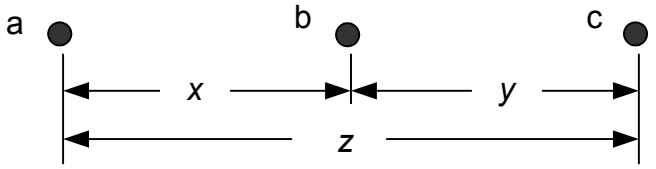

Figure 28 —Line with horizontal construction

In the configuration shown in Figure 28, the distance x is the same as y and the mutual impedances Z_x and Z_y are expected to be equal. However, because of the wider spacing z, Z_z will not have the same value. The matrix for a 162-km untransposed 500-kV line with flat construction is given in Equation (41). The impedance is in per unit on a 500-kV 1000-MVA base:

$$Z = \begin{pmatrix} 0.048 + j0.432 & 0.036 + j0.181 & 0.036 + j0.147 \\ 0.036 + j0.181 & 0.048 + j0.432 & 0.036 + j0.181 \\ 0.036 + j0.147 & 0.036 + j0.181 & 0.048 + j0.432 \end{pmatrix} \tag{41}$$

The symmetrical component matrix in this case is shown in Equation (42):

$$Z_{sym} = A\,Z\,A^{-1} = \begin{pmatrix} 0.12 + j0.771 & 0.01 + j0.06 & 0.01 + j0.06 \\ 0.01 + j0.06 & 0.012 + j0.262 & 0.019 + j0.11 \\ 0.01 + j0.06 & 0.019 + j0.11 & 0.012 + j0.262 \end{pmatrix} \tag{42}$$

In this case, the off-diagonal terms are not zero, indicating that there is coupling between the sequence networks for all types of faults. The per-unit calculation of a three-phase fault shows the effect of nontransposition on relay reach:

$$Z1a = \frac{V_a - V_b}{I_a - I_b} \qquad Z1b = \frac{V_b - V_c}{I_b - I_c} \qquad Z1c = \frac{V_c - V_a}{I_c - I_a}$$

$$\left|\frac{Z1a}{Z_{a1}}\right| = 0.952 \qquad \left|\frac{Z1b}{Z_{a1}}\right| = 0.946 \qquad \left|\frac{Z1c}{Z_{a1}}\right| = 1.085$$

The calculation shows that the fault locator for phase A and phase B overreaches by 4.8% and 5.4% respectively, while the Phase c mho element underreaches by 8.5%. Similar errors are introduced for unbalanced faults.

5.13 Comparison of one- and two-terminal impedance-based methods

5.13.1 Background

Since there is a great deal of experience with one-terminal fault location estimation, much is known about the accuracy and limitations to the effectiveness of these fault locators. In general, it can be said that the one-terminal fault location provides a good estimate if

a) Configuration is a fully transposed overhead line

b) Fault type is selected correctly

c) Strong source behind the measuring device for unbalanced faults exists (this tends to reduce remote source contribution, thus, reducing reactance effect error)

d) Little or no zero-sequence mutual coupling exists

5.13.2 500-kV system example: reactance method versus Takagi method

In the example in Figure 29, ground faults were simulated on a 162 km, 500-kV transposed transmission line.

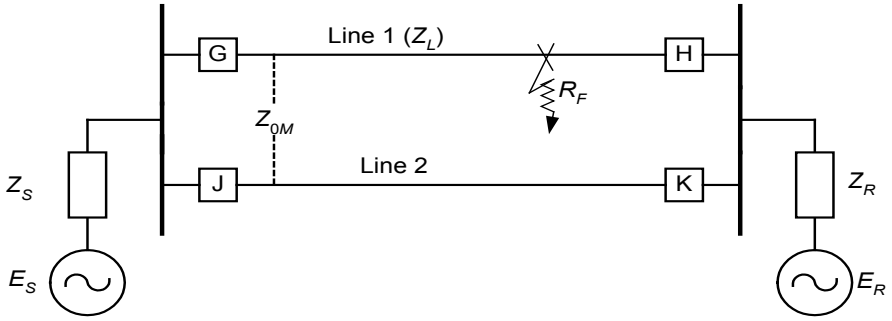

Z_{1S} = 50 ∠90° Ω

Z_{0S} = 150 ∠90° Ω (or 180 ∠56.3°)

Z_{1R} = 19.98 ∠90° Ω

Z_{0R} = 29.99 ∠90° Ω

Z_{1L} = 65.67 ∠87.36° Ω

Z_{0L} = 195.1 ∠81.17° Ω

Z_M = 102.5 ∠74.88° Ω (when present)

All impedances are in primary ohms.

System voltage: 525 kV

E_S = 1.0 ∠δ per unit

E_R = 1.0 ∠0° per unit

R_F = variable

δ = variable

Line length = 162 km

Figure 29 —500-kV system example

Fault studies were used to obtain the steady-state values of current and voltage for single line-to-ground faults with various system and fault resistances. The effect of zero-sequence mutual coupling was added for examples (b), (d), and (e) in Figure 30 and the source was changed to a nonhomogeneous system for examples (f) and (g).

The current and voltage values from the fault study were then used to evaluate the performance of a theoretical reactance-type fault locator and a theoretical Takagi fault locator. The reactance-type fault location estimation was evaluated using Equation (9); the Takagi by Equation (13). The results are summarized in Figure 30. In all of these cases the error is calculated using the error definition in subclause 2.1 and the theoretical two-terminal fault location estimate would have produced zero error.

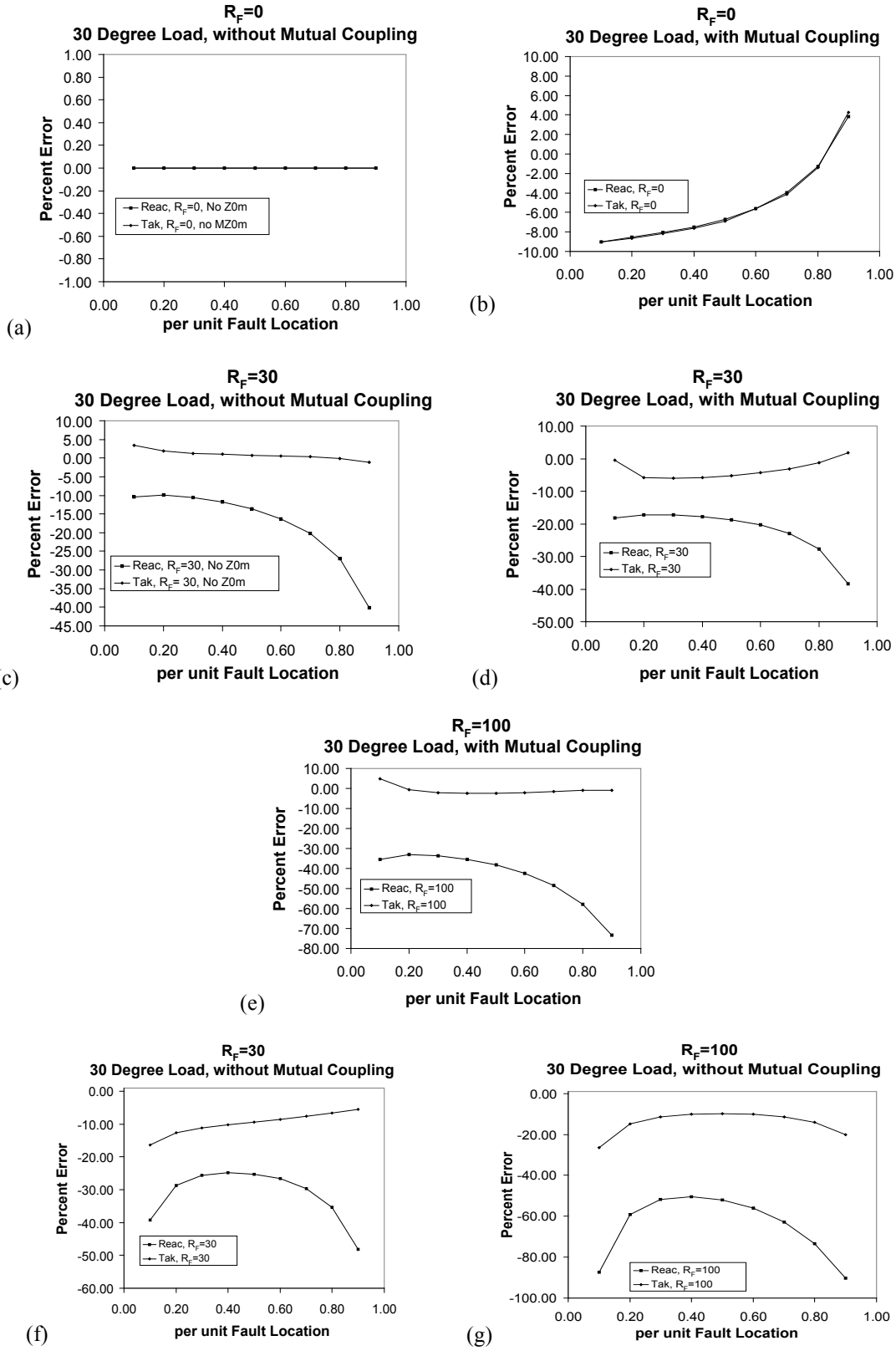

Figure 30 — (a–e) Plot of percent error of one-terminal fault location algorithms; (f–g) nonhomogeneous system

The charts in Figure 30 clearly show that the Takagi algorithm is superior to the reactance algorithm when fault resistance is included. Both algorithms are affected by the zero-sequence mutual coupling.

There are exceptions to the results of this example, however. Based on different system configurations, the reactance algorithm can, occasionally, produce a better result than the Takagi algorithm. But most often, the Takagi or similar algorithms provide superior results.

Note also that some sources of error cause the fault location estimate to be too high, others too low, or varying high or low depending on fault location. The result is that, in some cases, the sources of error can cancel each other out.

To demonstrate the effects of an increase in the nonhomogeneity of the system, the zero-sequence source impedance for source S was changed to 180 Ω at 56.3°. Increasing the nonhomogeneity of the system increases the errors in both the reactance and Takagi algorithms. For the example chosen, the effect on the reactance algorithm is substantial.

5.13.3 69 kV system example: one-terminal reactance method versus two-terminal method

In the example in Figure 31, ground faults were also simulated at different locations along a 29.4 km long transposed transmission line for a different network condition.

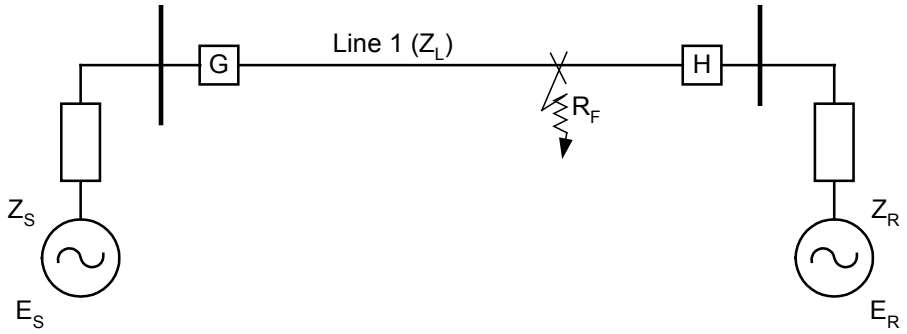

Z_{1S} = 3.75 ∠86° Ω

Z_{0S} = 11.25 ∠86° Ω

Z_{1R} = 12.0 ∠80° Ω

Z_{0R} = 36.0 ∠80° Ω

Z_{1L} = 15 ∠77° Ω

Z_{0L} = 50 ∠73° Ω

System voltage: 69 kV

E_S = 1.0 ∠δ per unit

E_R = 1.0 ∠0° per unit

R_F = variable

δ = 10°

Line length = 29.4 km

All impedances are in primary ohms.

Figure 31 —69 kV system example

The two-terminal algorithms do not introduce any error (even for the fault resistance equal to 100 Ω), while the error for the one-terminal algorithm can be substantial for a fault (even close to the bus) with a high fault resistance. The error may be very large for faults close to the remote end. In this example, the sources are assumed to be fixed with no mutual impedance present (see Figure 32).

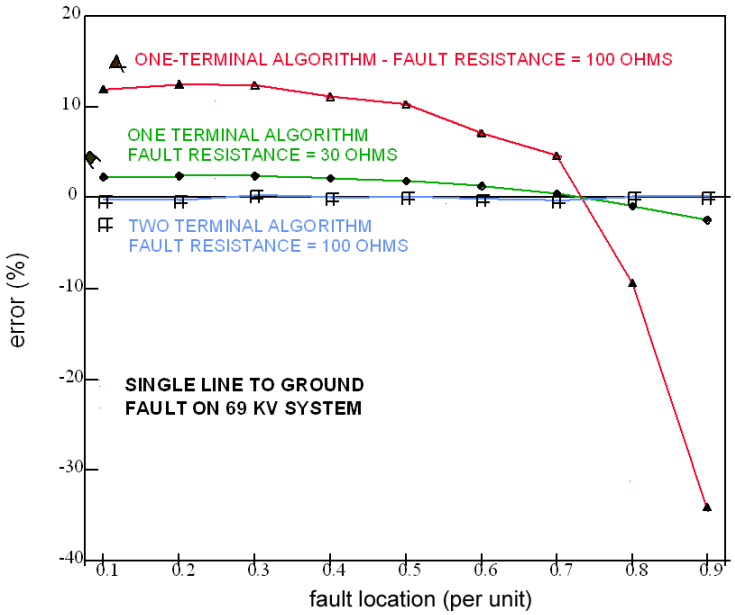

Figure 32 —Comparison between one- and two-terminal impedance-based algorithms for an example 69 kV line

Overall benefits of two-terminal data algorithms are

a) Fault resistance and load flow have no effect

b) Outside system has no effect

c) Mutual coupling has no effect

d) Fault type identification is not needed

e) Pre-fault data is not needed

f) Fault-path resistance can be calculated

5.14 Fault location for nonhomogeneous transmission lines

While some multi-ended fault location methods, such as the negative-sequence method shown in Tziouvaras, Roberts, and Benmouyal [B61], provide good results in applications where the X/R ratio of the transmission line is constant, they are not suitable for nonhomogeneous power transmission lines that consist of multiple sections with different X/R ratios. The nonhomogeneity of power lines can be caused by different tower configurations along the line or the combination of both overhead and underground cable line sections, as illustrated in Figure 33. The latter is common in metropolitan areas where overhead lines are more difficult to construct than underground cables.

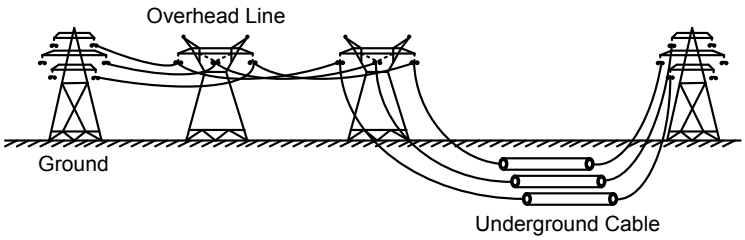

Figure 33 Nonhomogeneous power transmission line

To overcome the limitation of directly applying the existing double-ended fault location methods on nonhomogeneous lines, a method presented in Gong, et al. [B13] uses the profiles of the estimated voltage magnitude along the transmission line to determine the fault location. In this method, two voltage magnitude profiles can be constructed by using the line impedances of each line section and the voltage and current measurement from both terminals during the fault. Where the two voltage profiles intersect is the location of the fault. This method also applies to homogeneous lines. Figure 34 illustrates the main principle of this method. For unbalanced faults, the negative-sequence voltage magnitude profile is the preferred quantity to be used in this method. For three-phase balanced faults, the positive-sequence voltage magnitude profile should be used.

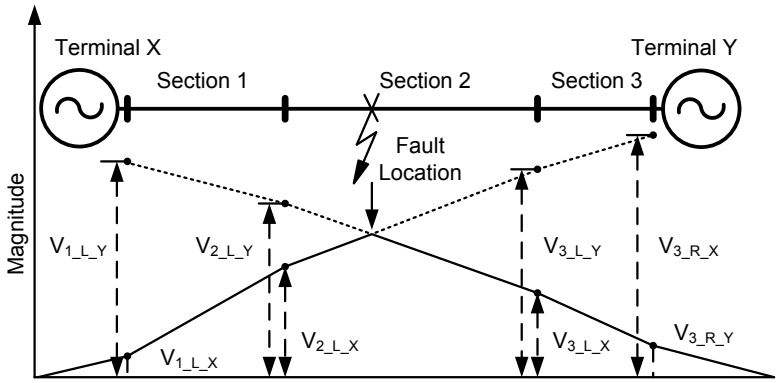

Figure 34 —Double-ended fault location method using voltage magnitude profiles

6. Traveling-wave techniques

6.1 Background

Traveling-wave methods may be used as an alternative for fault location. Recent improvements in data acquisition, time synchronization, and communication systems have increased the interest in this technology.

Traveling-waves (also called surges) on power lines arise from a number of causes, of which the most common are faults, switching operations, and lightning. Surges on overhead power lines travel at the speed

of light, approximately 3×10^8 m/s, and consist of a voltage wave and a current wave related through the surge impedance of the line, Z_0, which for all practical purposes can be considered to be a pure resistance, with a value between 200 Ω and 400 Ω, depending primarily on the operating voltage of the line. This relationship between the voltage and current waves exists at all points along the overhead line except at discontinuities such as line terminations and faults. At line terminations, the incident and reflected waves of voltage and current produce summated voltage and current waves. In per unit terms, and assuming a total of n lines, with the same value of Z_0, connected to a common bus bar, the summated waves on the line carrying the incident wave will result in:

$$\text{Summated voltage wave} = \frac{2}{1+n} \qquad \text{Summated current wave} = \frac{2n}{1+n} \tag{43}$$

From Equation (43) it can be seen that as the number of lines connected to a bus bar increases, the summated voltage wave will tend to zero, whereas the summated current wave will double. Also, current transformers (CTs) reproduce current transients in secondary quantities, but capacitive voltage transformers, being effectively tuned networks, do not. This analysis indicates that observation of current waves may be preferable to the selection of voltage waves, but in practice, both have been applied.

6.2 Data and equipment required

6.2.1 Data required

Traveling-wave methods typically rely on accurate timing information to provide accurate results. The traveling-wave method relies on calculation of time for the line disturbance to reach the end of the line. Essentially, when a disturbance occurs, very accurate time tagging must be done. Since the wave moves at the speed of light, by comparing the wave arrival time difference at each end, one can determine the distance to the source of the disturbance. This requires extremely accurate timing for calculation of fault location. Either voltage or current wave data can be used. The voltage portion of the traveling waveform tends to be reduced as the result of buses with lower impedance. On the other hand, the current waveform tends to double as the result of a constant current source characteristic.

The first data requirement is a standard time reference at both receiving terminals. Then some method of distinguishing which waveform must be used is required. The appropriate current waveform (or time tag in the voltage method) must be known to accurately calculate a fault location. From this point, a fault location can be calculated based on the precise wave arrival times on each end of the line. The main piece of data that must be known is the very precise time that the traveling wave reaches each end of the line. At this point, it is merely a matter of calculation.

6.2.2 Equipment required

The following equipment is necessary to locate faults using the traveling-wave method:

a) A very accurate time-stamping device on both ends of the line.

b) An appropriate sensor to detect the voltage or current, depending on the parameter used. In the case of the current wave, normal relaying accuracy current transformers are used. The secondary current transformer circuits then have the current pulses detected by clamp-on inductive sensors. In the case of detecting voltage pulses, capacitive potential transformers are utilized.

c) A communications circuit is required to transmit the time-stamped data back to a central location.

d) A computer capable of retrieving the remote data, distinguishing the appropriate waveform for the fault location calculation, and providing the appropriate calculations to the fault.

6.3 Accuracy limitations

6.3.1 Assumptions

Assumptions made in determining fault location include the following

a) The traveling waveform travels at the speed of light (velocity of propagation equals 3×10^8 m/s).

b) Discontinuities in the electrical system produce wave reflections. Each discontinuity can be used as calibration for the timing of the wave arrival at the receiving end of the line. Since the velocity of propagation is constant, the distance can be calculated quite accurately.

c) Time stamping must be very precise to make the system work.

d) The two-terminal method allows timing from the initiation of the short circuit, hence, reflected waves are not involved.

6.3.2 Factors that affect accuracy

Accuracy will vary depending on the following:

a) GPS-based traveling-wave fault locating systems where timestamp information is provided from both ends of the faulted transmission lines has proven to be very accurate. Operating results have shown accuracy on the performance of ± 300 meters, even for long lines.

b) Wave detection error due to interpretation of the transient is a major form of error. This error results from many transients and/or reflected transients appearing the same. This is especially true of lightning strikes. Lightning storms with multiple strokes can cause major confusion in terms of which transient was associated with which fault.

c) Stronger buses tend to dampen voltage transients. The result is lower fault locating accuracy.

d) GPS is a navigation system that provides an accurate standard time reference. Hence, any errors in this system are reflected into the ability to accurately locate faults. The Department of Defense intentionally builds a small amount of uncertainty into the system.

e) Current transformers provide reasonable reproduction of transients.

f) When utilizing the one-terminal form of the traveling-wave method, analysis of the waveforms has to be more sophisticated to identify appropriate reflections.

6.4 Traveling-wave methods

Following is an overview of traveling-wave methodology to determine the distance to a fault from a specified measuring point on a power system. When a fault occurs on a power system, high-frequency waves (impulses) called a travelling wave are generated. These travelling waves propagate away from the fault point in both directions toward the terminals of the line at velocities very near to the speed of light. By detecting these impulses and determining the time difference between the arrival of an impulse and its reflection or by comparing the arrival times of the two impulses (wave fronts) at the respective terminals of a line, the locations of a fault can be determined if the length and propagation velocity of the line are known.

Five types of traveling-wave fault locators exist. These are generally referred to as Type A, B, C, D, and E respectively. Following is a brief explanation of each type of traveling-wave fault locator.

Type A traveling-wave fault location is a passive single-ended fault location method and it measures the time difference between the arrival of the first wave front and its reflection. The fault location is then equivalent to half of this time difference between the arrival of the first wave and its reflection, if the propagation velocity of the travelling wave in the transmission line is known the distance to fault is calculated as follows:

$$D_{fault} = v_p \times \frac{\Delta t}{2} \tag{44}$$

where

v_p is the propagation velocity of the traveling wave in the transmission line

Δt is the time difference in the arrival of the first traveling wave and its reflection

Figure 35 is a sketch of a lattice diagram showing the principal of operation of this method.

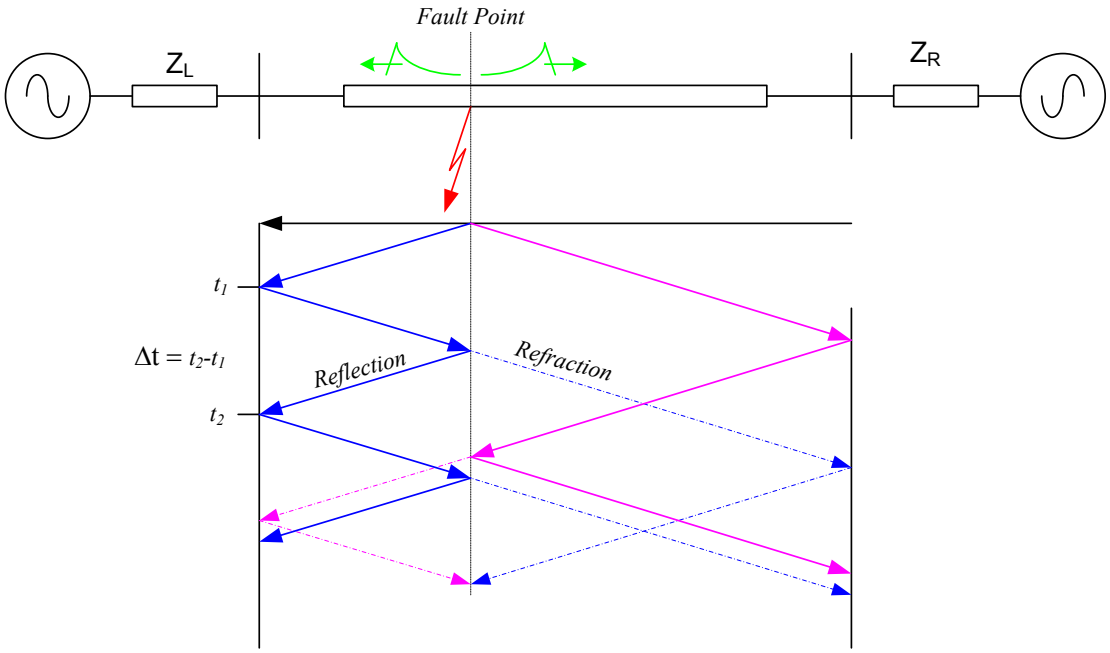

Figure 35—Lattice diagram showing the reflections and refractions caused by the traveling waves when a fault is present on a power system

For simplicity, this lattice diagram does not show the traveling waves transmitted (refracted) at the terminals. This method is appealing as it does not depend on the information from the remote terminal. However, identifying the reflections is a major challenge. As shown in the lattice diagram the reflections can be arriving from the fault or the remote terminal in addition, reflections can return from the circuits behind the terminals.

Type B is a passive dual ended fault location method. This method measures the time difference between the arrival of the traveling waves at the terminals of the line. A timer is started when the traveling wave arrives at the local terminal and stopped when a stop signal is received by the remote terminal. The remote terminal sends the stop signal when the traveling wave arrives at the remote terminal. Since the delay time to send the stop signal between the local and remote terminal is known this time can be subtracted from the

total difference time and the resultant difference is then the difference in time for the arrival of the two wave fronts at the terminals of the line. The time difference is then used to compute the distance to fault as follows:

$$D_{fault} = \frac{L}{2} + \frac{v_p \times \Delta t}{2} \tag{45}$$

where

Δt is the time difference in the arrival of the traveling waves at the local and remote terminals

L is the length of the transmission line

v_p is the propagation velocity of the traveling wave in the transmission line

Type C is an active single-ended method that injects an impulse into the line when a fault is detected, this method is also known as time domain reflectometery (TDM). This is very similar to the method used at present to detect faults in underground cables. The distance to fault is calculated by measuring the difference in time between the injection of the impulse and the arrival of the reflection. The distance to fault is calculated in a fashion similar to the one used for the Type A method.

Type D requires high accuracy time tagging at all the terminals of the line and telecommunication between the different traveling-wave device and a central unit. High accuracy time tagging (accuracy of less than 1 microsecond) is realized via time synchronized clocks at all terminals of the line. When the traveling wave arrives at a line terminal it is time stamped. The distance to fault is calculated in a variety of different ways, one method being very similar to that used for Type B.

Type E is a single-ended mode that uses the transients created when a line is re-energized by closing a circuit breaker at one line terminal. The method is equivalent to the impulse current method of fault location widely used on underground cables. Type E can be used to locate permanent faults, including open circuit conductors, where little or no fault current is flowing, and additionally can be used to measure the electrical length of healthy lines.

When applying fault locators based on Type D traveling waves recorded at all line terminals are sent to a central processing unit where the data from all the terminals is analyzed and the fault location is reported. A surge detector is used to trigger the recording with a defined pre-trigger and post-trigger data window. The data sampling resolution and time accuracy drives the accuracy of the fault location. The waves are seen in both voltage and current signals, it is important that the device/ transducer acquiring the signal has adequate bandwidth to capture the high-frequency impulse. Figure 36 shows the phase currents captured from both terminals of a 130-mile transmission line from a simulated power system in using the Alternate Transients Program (ATP). A fault is simulated on phase C at 35.55 miles; note that the impulse or step is dominant at the terminal closer to the fault.

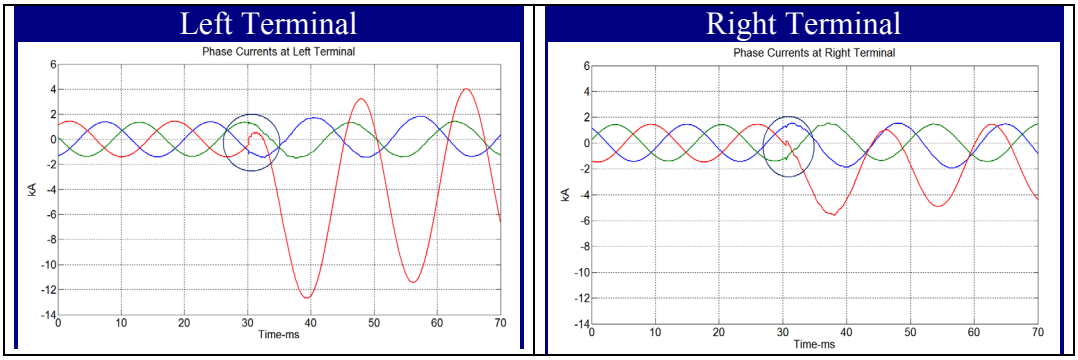

Figure 36—Phase currents captured at either terminals of the line for a ground fault

Estimating the fault location using these waveforms directly is possible by processing the signals using a high-pass filter to remove the nominal system frequency component. The time stamps corresponding to the wave front are recorded and used to compute the fault location. Figure 37 shows the processed signals along with time stamps of the wave front.

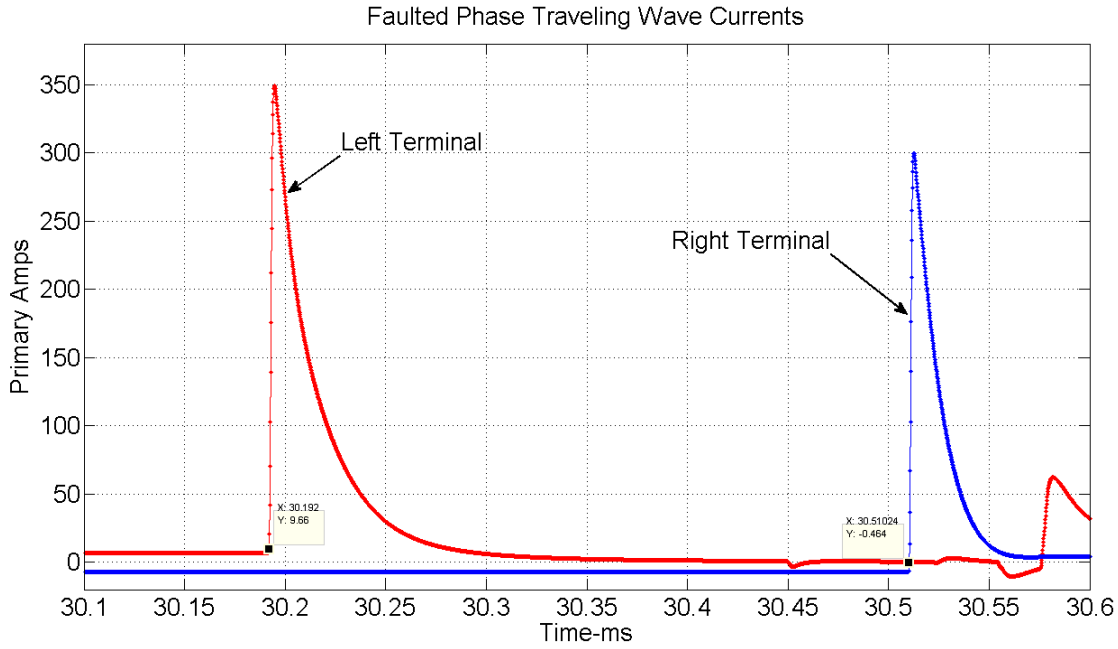

Figure 37—Traveling-wave current signals with time stamps corresponding to the wave-front

The time difference measured along with the line length and propagation velocity is used to compute the fault location. The propagation velocity for this example is 0.993 × speed of light, this value is calculated based on the traveling waves captured during line energization with the right terminal open.

$$D_{fault} = \frac{130\,\text{mi}}{2} + \frac{0.993 \times c \times \left(30.1920008 - 30.5102393\right) \times 10^{-3}}{2} \tag{46}$$

where

c is the speed of light in mi/s

7. Other techniques

7.1 Methods using synchronized phasors

Recent research in the use of synchronized phasors indicates they can be useful for application in fault locating. At present, these methods require the availability of GPS receivers or other equipment, and would be more costly than an unsynchronized approach. There are a number of references that suggest using synchronized phasors for two-terminal fault location (i.e., Girgis, Hart, and Peterson [B10], Hart, Novosel, and Udren [B15], Kezunovic [B24], and Lawrence, Cabeza, and Hochberg [B31]). The authors in Lawrence, Cabeza, and Hochberg [B31] use ABCD parameters to define the transmission line and derive equations for the fault location. Different equations are derived based on the fault type and Newton's

technique for nonlinear equations is used to derive the distance to the fault. The use of both synchronized and unsynchronized phasors was suggested in reference (Girgis, Hart, and Peterson [B10]). The algorithm modeled the line using the three-phase impedance matrix and, if present, the synchronization error. The unknown fault location and synchronization error were derived in a matrix format, and the equations were solved using the least squares technique (nonlinear least squares if the synchronization error was included). A technique that employed synchronized phasors and the positive-sequence impedance was tested (Hart, Novosel, and Udren [B15]). Utilizing synchronized measurements to solve for the fault location using a time domain technique was also suggested (Kezunovic [B24]).

7.2 Methods requiring time-tagging of the events

One approach utilizes pre-fault phasor estimates for two-terminal fault location. The pre-fault phasors are compared to determine the synchronization error between the two ends. Using the synchronization error, the fault location can be calculated (Schweitzer [B54]). This approach requires the user to manually specify the pre-fault data, compute the synchronization error, and compute the fault location. This approach is not applicable for faults without pre-fault load (e.g., reclosing into a fault). Another approach utilized the post-fault phasors in solving for the fault location (Sachdev and Agarwal [B48]). The voltage drop equations are solved using Cartesian coordinates, resulting in a quadratic equation for the unknown synchronization error. After using the quadratic equation to solve for the synchronization error, the fault location equations for each fault type have been developed. Positive- or negative-sequence components can be used to reduce mutual coupling effects (Novosel, et al. [B38]). The method does not require pre-fault data and fault type selection.

It should be noted that for all of these techniques, real-time communication is not required. While some require accurately time-stamped data, all analysis can be done off-line. It should be noted that the unsynchronized two-terminal algorithms can be used with synchronized data. The unsynchronized algorithm may provide improved results if there are errors due to different sampling rates or phase shifts introduced by the different recording devices and transducers.

8. Conclusion

Utilities have used many methods to help identify the correct fault location. Customer calls, line inspection, fault study data, digital fault recorders, and microprocessor-based relays are used to provide faster, more accurate results.

There has been a great deal of field experience with impedance-based fault locating methods, particularly on transmission lines. One-terminal methods produce decent performance, but are subject to many sources of error, including the effect load and fault resistance; zero-sequence mutual coupling caused by parallel lines; accuracy limits of system parameters, especially Z_0; incorrect fault identification; and other factors. Two-terminal methods correct many of these errors. Short duration faults and faults on lines that are not fully transposed can affect fault locating accuracy for both one- and two-terminal methods. Two-terminal methods require additional data to be communicated and analysis or software to make the calculations.

Traveling-wave methods show much promise where the time synchronization and other equipment is available to implement.

Distribution fault location remains a challenge because of the broad topography of modern distribution systems, many laterals, and varying conductor sizes.

This document aims at providing important guidance to engineers and operators in assisting them in determining fault locations on the power system.

Annex A

(informative)

Bibliography

Bibliographical references are resources that provide additional or helpful material but do not need to be understood or used to implement this standard. Reference to these resources is made for informational use only.

[B1] Aggarwal, R. K., D. V. Coury, A. T. Johns, and A. Kalam, "A Practical approach to accurate fault location on extra high voltage teed feeders," *IEEE Transactions on Power Delivery*, vol. 8, no. 3, pp. 874–883, July 1993.[3,4]

[B2] Bascom, E. C. III, D. W. Von Dollen, and H. W. Ng, "Computerized underground cable fault location expertise," *Proceedings of the IEEE Power Engineering Society Transmission and Distribution Conference*, Chicago, IL, Apr. 10–15, 1994.

[B3] Carson, J. R., "Wave propagation in overhead wires with ground return," *Bell Systems Technical Journal,* vol. 5, pp. 530–554, 1926.

[B4] Dong, Y., C. Zheng, and M. Kezunovic, "Enhancing accuracy while reducing computation complexity for voltage-sag-based distribution fault location," *IEEE Transactions on Power Delivery*, vol. 28, no. 2, pp. 1202–1212, Apr. 2013.

[B5] Eriksson, L., M. Saha, and G. D. Rockfeller, "An accurate fault locator with compensation for apparent reactance in the fault resistance resulting from remote-end infeed," *IEEE Transactions on Power Systems*, vol. PAS-104, no. 2, pp. 424–436, Feb. 1985.

[B6] Fecteau, C., "Accurate fault location algorithm for series-compensated lines using two-terminal unsynchronized measurements and Hydro-Quebec's field experience," *Western Protective Relay Conference, WPRC 2006*, Spokane, WA, Oct. 17–19, 2006.

[B7] Fecteau, C., D. Larose, and C. Deguire, "Nouveaux algorithmes de localisation de defauts et experience sur le reseau de transport d'Hydro-Quebec," *Study Committee B5 Colloquium,* Sept. 30–Oct. 1, 2003, Sydney, Australia (in French).

[B8] Fedirchuk, D. J., and P. Sheedy, "Utility sponsored development of a low cost power line monitor and fault locator," *Transactions of the Engineering and Operating Division of the Canadian Electrical Association*, Paper No. 89-TR-249, Report No. CEA-CE04228, vol. 28, Pts. 1–5.

[B9] Girgis, A. A., C. M. Fallon, and D. L. Lubkeman, "A fault location technique for rural distribution feeders," *IEEE Transactions on Industry Applications*, vol. 29, no. 6, pp. 1170–1175, Nov./Dec. 1993.

[B10] Girgis, A. A., D. G. Hart, and W. Peterson, "A new fault location technique for two- and three-terminal lines," *IEEE Transactions on Power Delivery*, vol. 7, no. 1, pp. 98–107, Jan. 1992.

[B11] Goldsworthy, D. L., "A linearized model for MOV-protected series capacitors," *IEEE Transactions on Power Systems*, vol. 2, no. 4, pp. 953–958, Nov. 1987.

[B12] Gong, Y., and A. Guzmán, "Integrated fault location system for power distribution feeders," proceedings of the IEEE Rural Electric Power Conference, Milwaukee, WI, Apr. 2012.

[B13] Gong, Y., M. Mynam, A. Guzmán, G. Benmouyal, and B. Shulim, "Automated fault location system for nonhomogeneous transmission networks," proceedings of the 65th Annual Conference for Protective Relay Engineers, College Station, TX, Apr. 2012.

[3] The IEEE standards or products referred to in this clause are trademarks of the Institute of Electrical and Electronics Engineers, Inc.
[4] IEEE publications are available from the Institute of Electrical and Electronics Engineers, Inc., 445 Hoes Lane, Piscataway, NJ 08854, USA (http://standards.ieee.org/).

[B14] Gopalakrishnan, A., M. Kezunovic, S. M. McKenna, and D. M. Hamai, "Fault location using distributed paramater transmission line model," *IEEE Transactions on Power Delivery*, vol. 15, no. 4, pp. 1169–1174, Oct. 2000.

[B15] Hart, D., D. Novosel, and E. Udren, "Application of synchronized phasors to fault location analysis," Applications of Synchronized Phasors Conference, Washington, DC, 1993.

[B16] IEEE Std 1159.3™-2003, IEEE Recommended Practice for the Transfer of Power Quality Data.

[B17] IEEE Std C37.111™-1999, IEEE Standard Common Format for Transient Data Exchange (COMTRADE) for Power Systems.

[B18] IEEE Std C37.2™, IEEE Standard Electrical Power System Device Function Numbers and Contact Designations.

[B19] IEEE Std C37.90™, IEEE Standard for Relays and Relay Systems Associated with Electric Power Apparatus.

[B20] IEEE Std C37.118.1™-2011, IEEE Standard for Synchrophasor Measurements for Power Systems.

[B21] IEEE Std C37.118.1a™-2014, IEEE Standard for Synchrophasor Measurements for Power Systems—Amendment 1: Modification of Selected Performance Requirements.

[B22] IEEE Std C37.118.2™-2011, IEEE Standard for Synchrophasor Data Transfer for Power Systems.

[B23] Johns, A. T., and S. Jamali, "Accurate fault location technique for power transmission lines," *IEEE Proceedings*, vol. 137, Pt. C, no. 6, pp. 395–402, Nov. 1990.

[B24] Kezunovic, M., "An accurate fault location using synchronized sampling at two ends of a transmission line," Applications of Synchronized Phasors Conference, Washington, DC, 1993.

[B25] Kezunovic, M., "Smart fault location for smart grids," *IEEE Transactions on Smart Grid*, vol. 2, no. 1, pp. 11–22, Mar. 2011.

[B26] Kezunovic, M., C.-C. Liu, J. R. McDonald, and L. Smith, "Automated fault analysis," IEEE Tutorial, July 2001.

[B27] Kezunovic, M., and B. Perunicic, "Fault location," *Wiley Encyclopedia of Electrical and Electronics Terminology*, vol. 7, New York: John Wiley, 1999, pp. 276–285.

[B28] Kezunovic, M., and B. Perunicic, "Automated transmission line fault analysis using synchronized sampling at two ends," *IEEE Transactions on Power Systems*, vol. 11, no. 1, Feb. 1996.

[B29] Kezunovic, M., and B. Perunicic, "Synchronized sampling improves fault location," *IEEE Computer Applications in Power*, vol. 8, no. 2, Apr. 1995.

[B30] Kezunovic, M., B. Perunicic, and J. Mrkic, "An accurate fault location algorithm using synchronized sampling," *Electric Power Systems Research Journal*, vol. 29, no. 3, pp. 161–169, May 1994.

[B31] Lawrence, D. J., L. Cabeza, and L. Hochberg, "Development of an advanced transmission line fault location system part II—Algorithm development and simulation," *IEEE Transactions on Power Delivery*, vol. 7, no. 4, Oct. 1992, pp. 1972–1983.

[B32] Lotfifard, S., M. Kezunovic, and M. J. Mousavi, "A systematic approach for ranking distribution systems fault location algorithms and eliminating false estimates," *IEEE Transactions on Power Delivery*, vol. 28, no. 1, pp. 285–293, Jan. 2013.

[B33] Lotfifard, S., M. Kezunovic, and M. J. Mousavi, "Voltage sag data utilization for distribution fault location," *IEEE Transactions on Power Delivery*, vol. 26, no. 2, pp. 1239–1246, Apr. 2011.

[B34] Luo, S., M. Kezunovic, and D. R. Sevick, "Locating faults in the transmission network using sparse field measurements, simulation data and genetic algorithm," *Electric Power Systems Research Journal*, vol. 71, no. 2, pp. 169–177, Oct. 2004.

[B35] Makki, A., R. Rothweiler, R. Orndorff, and G. B. Starling, "Double ended fault location application using IEEE Standard C37.114," *Proceedings of the 2013 Georgia Tech Fault and Disturbance Conference,* Atlanta, GA, May 2013.

[B36] Marttila, R. J., "Location of transient faults on high voltage transmission lines," *CEA Report ST-470*, Aug. 1994.

[B37] Novosel, D., B. Bachmann, D. G. Hart, Y. Hu, and M. M. Saha, "Algorithms for locating faults on series-compensated lines using neural network and deterministic methods," *IEEE Transactions on Power Delivery*, vol. 11, no. 4, pp. 1728–1736, Oct. 1996.

[B38] Novosel, D., D. G. Hart, E. Udren, and J. Garitty, "Unsynchronized two-terminal fault location estimation," *IEEE Winter Meeting*, paper 95 WM 025-7 PWRD, New York, NY, Jan. 1995.

[B39] Novosel, D., D. G. Hart, E. Udren, and A. Phadke, "Accurate fault location using digital relays," *International Conference on Plasma Science & Technology (ICPST),* Chengdu, China, pp. 1120–1124, Oct. 1994.

[B40] Novosel, D., A. G. Phadke, M. M. Saha, and S. Lindahl, "Problems and solutions for microprocessor protection of series-compensated lines," *Sixth Conference on Developments in Power System Protection*, Nottingham, UK, pp. 18–23, Mar. 1997.

[B41] Paithankar, S. and Y. Paithankar, "On line digital fault locator for overhead transmission line," *IEEE Proceedings*, vol. 126, no. 11, pp. 1181–1185, Nov. 1979.

[B42] Pereira, R. A. F., M. Kezunovic, and J. R. S. Mantovani, "Fault location algorithm for primary distribution feeders based on voltage sags," *International Journal on Innovations in Energy Systems and Power,* vol. 4, no. 1, Apr. 2009.

[B43] Pereira, R. A. F., L. G. W. Silva, M. Kezunovic, and J. R. S. Mantovani, "Improved fault location on distribution feeders based on matching during-fault voltage sags," *IEEE Transactions on Power Delivery*, vol. 24, no. 2, pp. 852–862, Apr. 2009.

[B44] Peterson, W., D. Novosel, D. Hart, T. W. Cease, and J. Schneider, "Tapping IEDs for transmission line fault location," *IEEE Computer Applications in Power,* Apr. 1999.

[B45] Phadke, A., M. Kezunovic, B. Pickett, M. Adamiak, M. Begovic, G. Benmouyal, R. Burnett, Jr., T. Cease, J. Goossens, D. Hansen, L. Mankoff, P. McLaren, G. Michel, R. Murphy, J. Nordstrom, M. Sachdev, H. Smith, J. Thorp, M. Trotignon, T. Wang, and M. Xavier, "Synchronized sampling and phasor measurements for relaying and control," *IEEE Transactions on Power Delivery*, vol. 9, no. 1, pp. 442–452, Jan. 1994.

[B46] Philippot, L., and J. C. Maun, "An application of synchronous phasor measurement to the estimation of the parameters of an overhead transmission line," *Fault Disturbance Analysis & Precise Measurements in Power Systems*, Arlington, VA, Nov. 1995.

[B47] Sabin, D. D., C. Dimitriu, D. Santiago, and G. Baroudi, "Overview of an automatic underground distribution fault location system," *IEEE Power & Energy Society General Meeting, 2009*, pp. 1–5, 26–30, July 2009.

[B48] Sachdev, M., and R. Agarwal, "A technique for estimating transmission line fault locations from digital impedance relay measurements," *IEEE Transactions on Power Delivery*, vol. 3, no. 1, pp. 121–129, Jan. 1988.

[B49] Sachdev, M. S., R. Das, and T. S. Sidhu, "Determining location of faults in distribution systems," *Proceedings of the IEE International Conference on Developments in Power System Protection*, Nottingham, UK, pp. 188–191, Mar. 25–27, 1997.

[B50] Saha, M. M., J. Izykowski, E. Rosolowski, P. Balcerek, and M. Fulczyk, "Accurate location of faults on series-compensated lines with use of two-end unsynchronized measurements," *IET 9th International Conference on Developments in Power System Protection, DPSP 2008*, Glasgow, UK, 2008.

[B51] Saha, M. M., J. Izykowski, E. Rosolowski, and B. Kasztenny, "A new fault locating algorithm for series-compensated lines," *IEEE Transactions on Power Delivery*, vol. 14, no. 3, pp. 789–797, July 1999.

[B52] Saha, M. M., K. Wikstrom, J. Izykowski, and E. Rosolowski, "Fault location in uncompensated and series-compensated parallel lines," *Proceedings of 2000 IEEE PES Winter Meeting*, Singapore, paper 16_05_01, Jan. 23–27, 2000.

[B53] Saha, M. M., K. Wikstrom, S. Lidstrom, and L. Kopari, "Implementation of new fault locating technique for series-compensated transmission lines," *CIGRE Colloquium*, Florence, paper S.C. 34–212, 1999.

[B54] Schweitzer, E. O. III, "Evaluation and development of transmission line fault-locating techniques which use sinusoidal steady-state information," *Ninth Annual Western Protective Relay Conference*, Spokane, WA, Oct. 1982.

[B55] Schweitzer, E. O. III, "A review of impedance-based fault locating experience," *Fifteenth Annual Western Protective Relay Conference*, Spokane, WA, Oct. 24–27, 1988.

[B56] Srinivasan, K. and A. St-Jacques, "A new fault location algorithm for radial transmission line with loads," *IEEE Transactions on Power Delivery*, vol. 4, no. 3, pp. 1676–1682, July 1989.

[B57] Stringfield, T. W., D. J. Marihart, and R. F. Stevens, "Fault location methods for overhead lines," *Transactions of the AIEE, Part III—Power Apparatus and Systems*, vol. 76, pp. 518–530, Aug. 1957.

[B58] Takagi, et al.; "Development of a new fault locator using the one-terminal voltage and current data," *IEEE Transactions on Power Apparatus and Systems*, vol. PAS-101, no. 8, pp. 2892–2898, Aug. 1982.

[B59] Tsuji, K., H. Yanagida, H. Sasaki, and S. Abe, "Development of fault characterization equipment (FCAREC) for power transmission lines," *IEEE Transactions on Power Delivery*, vol. 7, no. 1, pp. 133–138, Jan. 1992.

[B60] Turner, S., "Simple Techniques for Fault Location," *Proceedings of the 2002 Georgia Tech Protective Relay Conference,* May 2002.

[B61] Tziouvaras, D. A., J. Roberts, and G. Benmouyal, "New multi-ended fault location design for two- or three-terminal lines," *Development in Power System Protection*, Amsterdam, The Netherlands, Apr. 9–12, 2001.

[B62] Wiggins, C. M., "A novel concept for URD cable fault location," *IEEE Transactions on Power Delivery*, vol. 9, no. 1, pp. 591–597, Jan. 1994.

[B63] Yu, C. S., C. W. Liu, S. L. Yu, and J. A. Jiang, "A new PMU-based fault location algorithm for series-compensated lines," *IEEE Transactions on Power Delivery*, vol. 17, no. 1, pp. 33–46, Jan. 2002.

[B64] Zimmerman, K., and D. Costello, "Impedance-based fault location experience," *Proceedings of the 58th Annual Conference for Protective Relay Engineers*, College Station, TX, Apr. 2005.

[B65] Zocholl, S. E., "Symmetrical components: line transposition," http://www.selinc.com/techpprs/6090.pdf, Mar. 1999.

Annex B

(informative)

Additional information on series-compensated lines

Fault location in series-compensated lines depends to large extent on the place of installation of series capacitors (SCs) and the method of their overvoltage protection. Figure B.1 presents a line with banks of SCs installed in some distance *m* (p.u.) from the substation A. Overvoltage protection of SCs is performed here with metal oxide varistors (MOVs) connected in parallel. For such a transmission network, the voltage drops across the SCs and MOVs are not measurable at the substation. Fortunately, they can be estimated on the base of the locally available measurements. Both the deterministic and the artificial neural networks–based approaches for that purpose have been considered and deeply investigated in Peterson, et al. [B44]. Having estimated voltage drops across the SCs and MOVs, one can adapt the fault location algorithms designed for traditional (i.e., uncompensated lines) to locating faults in series-compensated lines. This is achieved by compensating the measured phase voltages for the estimated voltage drops.

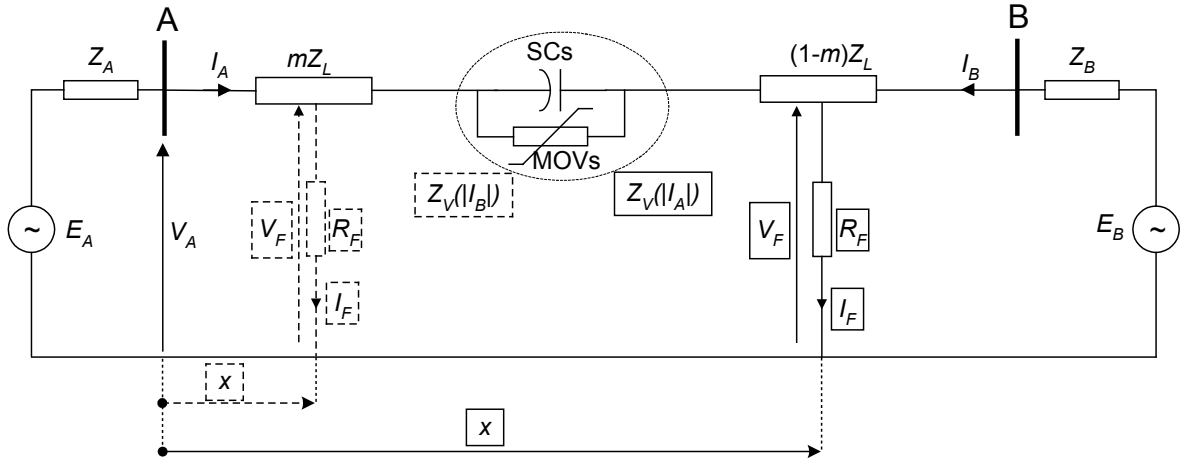

Faults (as seen from the substation A) and the relevant quantities are denoted:

- solid line boxes—fault behind the SCs and MOVs;
- dashed line boxes—fault in front of the SCs and MOVs.

Figure B.1—One-line diagram of a series-compensated line with two sources

Usage of the fundamental frequency equivalents as the other possibility for representing the SCs and MOVs has been proposed in Goldsworthy [B11] and applied in the fault location algorithm Saha, et al. [B51]. The SCs and MOVs are represented with the equivalent resistance (R_V) and reactance (X_V) being the nonlinear functions of amplitude of a current ($|I_V|$) entering the SC and MOV installation (Figure B.2). The fundamental frequency components of the signals (I_V,V_V) in both the circuits of Figure B.2 match each other.

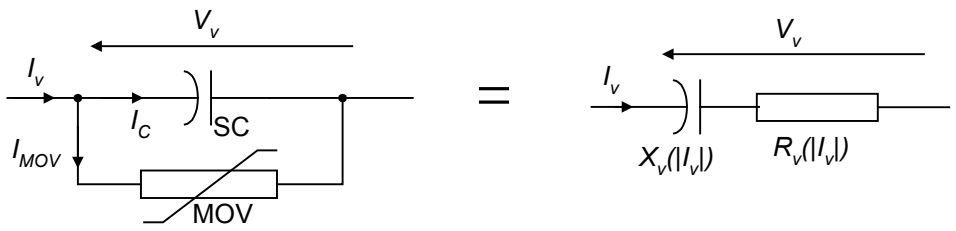

(a) original circuit (b) equivalent circuit

Figure B.2—Principle of fundamental frequency equivalencing of SC and MOV branches

Under unsymmetrical faults, which are the majority of the power system faults, amplitudes of phase currents are unsymmetrical, and in consequence the fundamental frequency equivalents in particular phases differ with respect to the amount of the equivalent resistance and reactance. The phase coordinates approach for the system description has been proposed to deal in a convenient way with such cases. In addition, a generalized fault model, covering different fault types, is used in this algorithm, Equation (B.1), as well:

$$I_F = \frac{1}{R_F} K_F V_F \tag{B.1}$$

where

V_F and I_F are vectors of voltages and currents at fault point

R_F is the aggregated fault resistance

K_F is the fault matrix built upon the type of fault

The location algorithm branches into two separate subroutines considering the two characteristic fault spots (Figure B.1):

a) SUBROUTINE 1—for faults behind the SCs

b) SUBROUTINE 2—for faults in front of the SCs

If the fault occurs behind the SCs (SUBROUTINE 1), the current flowing through the compensating bank (I_V) is directly measured by the fault locator (I_A) and the following matrix equations (see Equation (B.2) and Equation (B.3)) apply to the faulty network (Figure B.1):

$$E_A - E_B = \left[Z_A + xZ_L + Z_V\left(|I_A|\right)\right]I_A - \left[(1-x)Z_L + Z_B\right]I_B \tag{B.2}$$

$$V_A - V_F = \left[xZ_L + Z_V\left(|I_A|\right)\right]I_A \tag{B.3}$$

where

x is the distance to a fault (p.u.) ($p < \times < 1$)

The other quantities are marked in Figure B.1.

For the pre-fault network (the subscript *pre* denotes the pre-fault values), the following, as seen in Equation (B.4), holds:

$$E_A - E_B = \left[Z_A + Z_L + Z_V\left(\left|I_{A\_pre}\right|\right) + Z_B\right] I_{A\_pre} \tag{B.4}$$

The set of the above matrix equations is solved for x and R_F, which yields the simple quadratic equation:

$$Ax^2 + Bx + C - R_F = 0 \tag{B.5}$$

where

A, B, and C are the complex scalars determined with the system parameters and the local measurements

Resolving the above quadratic equation into the real and imaginary parts allows calculating the sought after fault distance (x).

On the other hand, in the case of a fault between the substation and the SCs (SUBROUTINE 2), the current flowing through the SCs and MOVs is not directly measured by the locator ($I_V = I_B \neq I_A$) and the following applies to the faulty network (Figure B.1):

$$E_A - E_B = \left(Z_A + xZ_L\right) I_A - \left[(1-x)Z_L + Z_V\left(\left|I_B\right|\right) + Z_B\right] I_B \tag{B.6}$$

$$V_A - V_F = \left(xZ_L\right) I_A \tag{B.7}$$

where

$0 < x < m$

In consequence, one also obtains the quadratic equation as for the SUBPROCEDURE 1, but the iterative numerical solution is required because the coefficients depend on the unknown amplitudes of the phase currents from the remote substation B.

The fault location algorithm has been implemented in one Swedish utility and is undergoing field tests on 400-kV series-compensated lines (Saha, et al. [B53]). Further extension of the algorithm for locating faults in series-compensated parallel lines is described in Saha, et al. [B52].

Consensus

WE BUILD IT.

Connect with us on:

Facebook: https://www.facebook.com/ieeesa

Twitter: @ieeesa

LinkedIn: http://www.linkedin.com/groups/IEEESA-Official-IEEE-Standards-Association-1791118

IEEE-SA Standards Insight blog: http://standardsinsight.com

YouTube: IEEE-SA Channel

IEEE
standards.ieee.org
Phone: +1 732 981 0060 Fax: +1 732 562 1571